Cell Biology:

Glycosylation in a mammalian expression system is critical for the production of functionally active leukocyte immunoglobulin-like receptor A3 protein

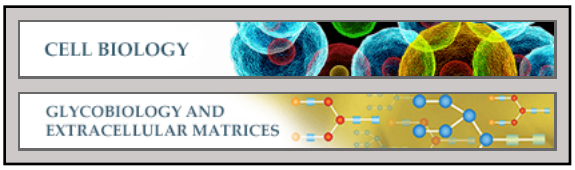

Terry H. Y. Lee, Ainslie Mitchell, Sydney Liu Lau, Hongyan An, Poornima Rajeaskariah, Valerie Wasinger, Mark Raftery, Katherine Bryant and Nicodemus Tedla

J. Biol. Chem. published online September 30, 2013

JBC Papers in Press. Published on September 30, 2013 as Manuscript M113.478578
The latest version is at http://www.jbc.org/cgi/doi/10.1074/jbc.M113.478578

Glycosylation in a mammalian expression system is critical for the production of functionally active Leukocyte Immunoglobulin-like Receptor A3 protein.

Terry H. Y. Lee[1], Ainslie Mitchell[1], Sydney Liu Lau[3], Hongyan An[1], Poornima Rajeaskariah[1], Valerie Wasinger[3], Mark Raftery[3], Katherine Bryant[1,2*], Nicodemus Tedla[1*]

[1]Inflammation and Infection Research Centre, School of Medical Sciences, University of New South Wales, Sydney, Australia, [2]South Western Sydney Clinical School, University of New South Wales, Australia, [3]Bioanalytical Mass Spectrometry Facility, Mark Wainwright Analytical Centre, The University of New South Wales, Australia.

Running title: LILRA3 binds monocytes and inhibits LPS-mediated TNFα production

To whom correspondence should be addressed: A/Prof Nicodemus Tedla or Dr Katherine Bryant, Inflammation and Infection Research Centre, University of New South Wales, Sydney, 2052 Australia. Telephone: (02) 9385 2919. Fax: (02) 9385 1389. E-mail: n.tedla@unsw.edu.au; katherine.bryant@unsw.edu.au
*Authors contributed equally.

Keywords:
Leukocyte immunoglobulin-like receptor A3, monocytes, ligand binding, recombinant proteins, N-glycosylation, TNFα

Background: LILRA3 is a soluble receptor abundantly present in human serum with unknown functions.
Result: Optimally glycosylated recombinant LILRA3 protein produced only in mammalian system binds potential ligands and suppresses monocyte function.
Conclusion: LILRA3 suppresses LPS-mediated TNF production, suggesting it is a new anti-inflammatory protein.
Significance: This work provides first insight into the biochemical characteristics and functions of LILRA3.

SUMMARY

The leukocyte immunoglobulin-like receptor A3 (LILRA3) is a member of highly homologous activating and inhibitory receptors expressed on leukocytes. LILRA3 is a soluble receptor of unknown functions but predicted to act as a broad antagonist to other membrane-bound leukocyte immunoglobulin-like receptors (LILRs). Functions of LILRA3 are unclear primarily due to lack of high quality functional recombinant protein and due to insufficient knowledge regarding its ligand(s). Here, we expressed and characterised recombinant LILRA3 (rLILRA3) proteins produced in 293T cells, in *E. coli* and *Pichia pastoris*. We found the purified rLILRA3 produced in the mammalian system was the same size as a 70kDa native macrophage LILRA3. This is 20kDa larger than the calculated size, suggesting significant post-translational modifications. In contrast, rLILRA3 produced in *E. coli* was similar size to the unprocessed protein but yeast produced protein was 2-4 times larger than the unprocessed protein. Treatment with PNGase F reduced the size of the mammalian and yeast produced rLILRA3 to 50kDa, suggesting most modifications are due to glycosylation. Consistent with this, mass spectrometric analysis of the mammalian rLILRA3, revealed canonical N-glycosylation at the predicted N_{140}, N_{281}, N_{302}, N_{341} and N_{431} sites. Functionally, only mammalian expressed rLILRA3 bound onto the surface of monocytes with high affinity and importantly, only this significantly abrogated LPS-induced TNFα production by monocytes. Binding to monocytes was partially blocked by β-lactose, indicating optimally glycosylated LILRA3 might be critical for ligand binding and function. Overall, our data demonstrated for the first time that LILRA3 is a potential new anti-inflammatory protein and optimal glycosylation is required for its functions.

Leukocyte Immunoglobulin-like Receptor-(LILR) A3 belongs to a family of highly homologous activating and inhibitory receptors primarily co-expressed on mono-myeloid leukocytes and are increasingly recognised to regulate innate immune responses (1). Activating LILRs (LILRA) have a

short cytoplasmic tail that links to the intracellular immunoreceptor tyrosine-based activation motifs (ITAMs) of the Fc receptors common-γ chain and transduces activating signals via protein tyrosine kinases (2). Inhibitory LILRs (LILRB) have a long cytoplasmic tail that contains two to four immunoreceptor tyrosine-based inhibitory motifs (ITIMs) that recruit SH2-containing inhibitory phosphatases such as SHP-1 (3). Co-engagement by shared ligands may regulate the threshold and amplitude of leukocyte activation. LILRA3 is a soluble protein with unknown function but bears close sequence homology to the extracellular domains of activating LILRA1 and LILRA2, thus may act as a soluble antagonist (4,5). We previously showed that LILRA3 is abundantly present in normal serum and is significantly increased in sera of patients with rheumatoid arthritis (6). We proposed that LILRA3 may antagonise the effects of LILRA2 which is increased in highly inflamed synovial tissue (7). Interestingly, absence of a functional allele due to a natural gene deletion (4) has been shown to strongly associate with increased incidence of multiple sclerosis (8,9) and Sjogren's syndrome (10), both characterised with excessive inflammation, suggesting LILRA3 may play key role in the pathogenesis of chronic inflammatory diseases. Consistent with this LILRA3 is strongly up-regulated by the anti-inflammatory cytokine IL-10 and down-regulated by pro-inflammatory cytokine TNFα (6). However, the exact *in vivo* and *in vitro* functions of LILRA3 are poorly established, primarily due to inadequate knowledge about its ligand(s). The major impediments for comprehensive identification of high affinity LILR ligand(s) and understanding functions *in vivo* are lack of properly folded and post-translationally modified, full length recombinant LILR proteins and absence of robust protocols capable of simultaneously identifying ligands and/or co-ligands. The former is particularly relevant since LILRs are predicted to be highly glycosylated and have multiple disulphide bonds thus recombinant LILRs produced in non-eukaryotic cells is likely to be unsuitable for functional assays.

In this report we produced high quality, properly folded, full length rLILRA3 protein with or without C-terminal placental alkaline phosphatase tag in a mammalian system using 293T cells. More importantly, rLILRA3 protein produced in 293T cells was successfully used to screen specific binding of this protein to various cell types. We show for the first time that LILRA3 strongly and specifically bound onto the surface of the monocytic cell line U937 and primary peripheral blood monocytes, suggesting expression of LILRA3 ligand(s) on these cells. Moreover, treatment of primary monocytes with purified mammalian recombinant LILRA3 significantly suppressed LPS-mediated TNFα production indicating functional interaction of LILRA3 with its yet uncharacterised ligand. By contrast, full length rLILRA3 produced in bacteria or yeast had poor binding and failed to suppress LPS induced activation of monocytes. This variability in binding and function might be due to the optimal post-translational modification of the rLILRA3 produced in 293T cells. Indeed, rLILRA3 protein produced in 293T cells showed 5 N-glycosylation sites that likely have contributed to its superior ability to functionally bind to its potential ligand(s). Consistent with the latter, pre-treatment of cells with β-lactose partially abrogated binding of rLILRA3 to the surface of monocytes. Taken together, recombinant LILRA3 that can be used for screening and identification of its ligand(s) and characterisation of functions is best produced in higher eukaryote expression systems.

EXPERIMENTAL PROCEDURES

Cloning of LILRA3 cDNA into mammalian, bacteria and yeast expression vectors: Full length LILRA3 cDNA was amplified from PBMC mRNA and inserted into pCR2.1vector (Invitrogen, USA). This was used for further sub-cloning into mammalian (pAPtag-5; GenHunter, USA), bacteria (pET30/LIC, Novagen, USA) and yeast (pPICZβ; Invitrogen, USA) expression vectors. In brief, a full length LILRA3 without signal peptide was re-amplified using 5'-AAGCTTTAAGGACCCACGTGCAGGCAGG-3' forward and 5'-AAGCTTCCCACTCACCAGCCTTGGAGTC-3' reverse primers containing Hind III restriction sites. This was inserted into Hind III digested pAPtag-5 (GenHunter, USA) vector to generate mammalian rLILRA3 protein with heat resistant placental alkaline phosphatase and 6x histidine tags on its C-terminal (rLILRA3-APtag-His). Mammalian rLILRA3-His protein without APtag was generated by introduction of a new 6xHis sequence and a stop codon using 5'-CCGAAGCTTTAAGGACCCACGT-3' forward primer and 5'-GGCCTCGAGTCAATGATGATGATGATGATGCTCACCAGCCTTGGAG-3', reverse primers and directionally sub-cloned to pAPtag-5 vector, linearized with Hind III and Xho I.. To generate rLILRA3-His protein in *E. coli,* rLILRA3 without signal peptide was amplified using 5'-GACGACGACAAGACCAGGACCCACGTG-3'

forward primer and 5'-GAGGAGAAGCCCGGTCACCAGCCTTGG-3' reverse primer and ligated into pET30 EK/LIC expression vector (Novagen). rLILRA3-His was produced in yeast after sub-cloning of LILRA3 without signal peptide from pPIC9k vector using 5'-CCGCTCGAGAAAAGAGGGCCCCTCCCCAAGCCC-3' forward and 5'-CCACTCGTAGTAGTAGTAGTAGTAACTGAGCTCCGG-3' reverse primers and inserted to pPICZβ expression vector at XhoI cloning site. See Supp. Fig 1 for illustration of the recombinant proteins.

Production of secreted recombinant LILRA3 and placental alkaline phosphatase in a mammalian system: The LILRA3 with or without APtag in pAPtag-5 vector alone were stably transfected into, 293T cell line using Lipofectamine LTX reagent (Invitrogen), cultured in DMEM +10% FBS and selected with 300 µg/ml Zeocin (Invitrogen). During each weekly passage, secreted recombinant LILRA3-APtag-His and APtag-His alone were detected in culture supernatants using a simple alkaline phosphatase activity assay as described (11). Secreted fusion proteins were further confirmed by Western blotting 15 µl of culture supernatants using mouse anti-human placental alkaline phosphatase mAb (GenHunter, USA). Production of rLILRA3-His without APtag protein was detected in culture supernatants by Western blotting using mouse anti-human LILRA3 mAb (Abcam, USA). Cells that produced high level of recombinant LILRA3 proteins were gradually adapted to DMEM containing 1% FBS and selection maintained with 30 µg/ml of Zeocin. Cells were then grown to confluence in 1 litre of the serum minimized media and recombinant protein containing culture supernatants collected and debris removed by high speed centrifugation at 330 g for 30 minutes at 4°C followed by filtration with 0.22 µm filters. Culture supernatants were then buffer exchanged and concentrated to 150 ml in binding buffer (20 mM Tris pH 7.4, 150 mM NaCl, 5 mM imidazole) using Amicon ultrafiltration system (Amicon, USA) with a 30 kDa cut off membrane (Millipore, USA). Buffer exchanged proteins were loaded onto 1 ml cobalt immobilised metal affinity resin (Clontech, USA) and connected to BioLogic DuoFlow FPLC (Bio-Rad, USA). The column was then stringently washed at flow rate of 2 ml/min with 20 bed volumes of 20 mM Tris pH 7.4, 150 mM NaCl (wash buffer) containing 10mM imidazole for APtag-His column or wash buffer containing 20 mM imidazole for rLILRA3-APtag-His and rLILRA3-His columns. Finally proteins were stepwise eluted with 5x2 ml fractions of 20 mM Tris pH 7.4, 300 mM NaCl elution buffers containing 50 mM, 150 mM and 300 mM imidazole. rLILRA3-APtag-His and rAPtag-His proteins in each eluted fraction were quantitated by comparing placental alkaline phosphatase (AP) activity using AP standards (Sigma) and the purified rLILRA3 without APtag was quantitated using standard BCA assay (Pierce). Proteins were further quality controlled by silver staining of SDS PAGE, Western blots and their identities verified by mass spectrometry. Fractions that contained high concentration and high quality proteins were pooled, dialysed into sterile LPS-minimised TBS (20mM Tris, 150 mM NaCl, pH 7.4) and re-quantitated. The resulting estimates of specific activity for the dialysed rLILRA3-APtag-His and rAPtag-His proteins were 960 U/mg and 1500 U/mg respectively. The concentration of the dialysed rLILRA3 protein without APtag-His was 0.4µg/ml. A total of 750 µg, 1000 µg and 400 µg of rLILRA3-APtag-His, rAPtag-His and rLILRA3-His respectively were produced from 1 litre of culture supernatants. These proteins were stable at 4°C for several months.

Production of recombinant LILRA3 in E. coli: LILRA3 in pET30 EK/LIC in BL21-DE3 with 50 µg/ml kanamycin selection was induced with 0.1 mM IPTG when reached optimal growth (OD_{600} 0.7-1.0). After overnight culture, the solubilisation and refolding of the recombinant protein from *E. coli* inclusion bodies were custom optimised by Protein'eXpert (France, Grenoble). In brief, bacteria cell pellet from 1 litre culture was lysed by sonication, washed twice with cold TBS and inclusion body solubilised in 40 mL of 50 mM Tris pH 8.5, 500 mM NaCl, 6 M guanidine and 10 mM β-mercaptoethanol overnight at 4°C. Solubilised protein was separated by centrifugation at 21 000 g for 30 minutes at 4°C and dialysed three times against 1 litre of buffer A each (50 mM Tris pH 8.5, 500 mM NaCl, 8 M urea, 1 mM glycine and 10 mM β-mercaptoethanol) using 10,000 Dalton cut off (Pierce). After dialysis, Sarkosyl was added to a final concentration of 0.3% and the solution was incubated for 4 hours at 4°C, sonicated 5 times and centrifuged at 21 000 g for 20 minutes. The soluble fraction was then loaded overnight at 4°C onto 1 ml cobalt containing metal affinity resin (Clontech) connected to FPLC (Bio-Rad). The column was washed with buffer A containing 0.3% sarkosyl and eluted with TBS buffer containing 150 mM imidazole (5x5 ml). Fractions of the eluted proteins with high purity and concentration were pooled (20 ml),

dialyzed three times over 12 hours against 1 litre of cold buffer B (50 mM Tris pH 8.5, 500 mM NaCl, 1 M urea, 25 mM $CaCl_2$, 10 mM β-mercaptoethanol and 0.1% Brij35) and finally centrifuged at 21 000 g for 20 minutes and the soluble fraction collected. This was then refolded by gradual dialysis into 4 changes (1 litre each) of cold 50 mM Tris pH 8.5, 200 mM NaCl, 1 mM DTT over a period of 18 hours and centrifuged at 21 000 g for 45 minutes to remove aggregated protein. The refolded soluble protein was quality controlled by HPLC and quantitated using BCA assay. Up to 15 mg of refolded protein was produced from 1 litre of bacteria culture. To prevent oxidation and aggregation, protein was stored under argon gas at -80°C in small aliquots of silicon-coated sealed vials at 1.3 mg/ml.

Production of recombinant LILRA3 in P. pastoris: LILRA3 in pPICZα-B vector was linearised with the restriction enzyme *PmeI* and transfected to *P. pastoris* (X33) by electroporation. Yeast strains showing single crossover recombination were selected to grow on minimal dextrose media and transformants showing Mut^+ phenotype picked and cultured on minimal methanol agar plates. rLILRA3 expressing colony was selected and grown in BMGY agar (100 mM potassium phosphate pH 6.0, 1% (w/v) yeast extract, 2% (w/v) peptone, 1.34% (w/v) YNB, 4x 10^{-5} % (w/v) biotin, 1% (v/v) glycerol, 200 µg/mL Zeocin) at 30°C until 1:10 diluted culture has an OD_{600} of 1.6-2.0. The culture media was changed to BMMY broth (1% (w/v) yeast extract, 2% (w/v) peptone, 100 mM potassium phosphate pH 6.0, 1.34% (w/v) YNB and 4x 10^{-5} % (w/v) biotin and cultured at 30°C for 24 hours. Cells were then induced with 0.5% (v/v) methanol every 24 hours until a total of 96 hours. The induced culture supernatant was harvested by removing cells with centrifugation at 3000 g for 20 minutes at 4°C and filtration using 0.22 µm cut off. The filtrate was then diluted 1:1 with binding buffer containing 50 mM sodium phosphate pH 8.0, 300 mM sodium chloride, 10 mM imidazole and loaded onto Nickel-MAC Cartridge column (Novagen) at a flow rate of 1 ml/min (AKTA Purifier, GE Pharmacia, USA). The column was washed with 40 bed volume of 50 mM sodium phosphate pH 8.0, 300 mM sodium chloride, 20 mM imidazole and eluted with 10 ml of elusion buffer (50 mM sodium phosphate pH 8.0, 300 mM sodium chloride, 250 mM imidazole). Approximately 250 µg protein was produced from 1 litre of yeast culture. The protein was stored at 4°C and used for up to 1 month.

Deglycosylation of recombinant LILRA3 produced in 293T and P. pastoris: To determine the extent of LILRA3 glycosylation, the mammalian and yeast produced recombinant proteins were treated with PNGase F according to the manufacturer's instructions (New England BioLabs, USA). In brief, 2 µL of 10x glycoprotein denaturing buffer was added to 2.5 µg of protein in 20 µL buffer and incubated at 95°C for 10 minutes. 3 µL of G7 reaction buffer, 3 µL of NP-40 and 1 µL (500U/µl) of PNGase F were then added to each reaction mix and samples incubated at 37°C for 1 hour. Changes in the deglycosylated rLILRA3 size and isoelectric focusing were determined by Western blotting of membranes from one and two dimensional SDS PAGE gels respectively and mass spectrometry.

Generation of primary human macrophages in vitro: Peripheral blood mononuclear cells from two healthy subjects were suspended at $5x10^6$/ml in RPMI 1640 containing 2mM L-Glutamine, 10U/ml penicillin and 100 mg/ml streptomycin (all from Invitrogen Life Technologies) and 10% autologous sera and seeded onto 6-well Costar® plates. Cells were incubated at 37°C, in a humidified atmosphere of 95% air and 5% CO_2 for 2 hours and non-adherent cells removed by two washes with PBS. The adherent cells were then cultured in 3ml of media supplemented with 25 ng/ml of GM-CSF (Invitrogen) for 3 days before washing twice in PBS and cultured for another 3 days in culture media without GM-SCF but containing 1:1000 dilution of Brefeldin A solution (BioLegend, San Diego USA). Cells were then washed twice with PBS and lysed in RIPA buffer (1% NP-40, 0.5% sodium deoxycholate, 50mM Tris (pH 8), 2 mM EDTA, 0.5 mM sodium orthovanadate, 5 mM sodium fluoride and protease inhibitors) and stored at -80°C until used for Western blotting to detect native LILRA3.

Western blotting and silver staining of one and two dimensional gels: For one dimensional gels, 10 µg of purified recombinant proteins or *in vitro* derived primary human macrophage (~$1x10^4$ cells) lysates were resolved into 10% SDS-PAGE under reducing and non-reducing conditions before and after treatment with PNGase. Gels were either silver stained or transferred onto PVDF membranes for Western blotting. In brief, PVDF membranes were rinsed with TBS and blocked in 5% skim milk in TBS for 1 hour at room temperature. Membranes were then probed with 1 µg/ml of either mouse anti-LILRA3 mAb (clone 2E9, Abnova) or rabbit anti-AP Ab (GenHunter) for 2 hours at room temperature, washed 4x 5 minutes with TBS+0.1% Tween 20. This was followed by incubation of membranes with

horseradish peroxidase (HRP) conjugated anti-mouse or anti-rabbit Abs (Bio-Rad) for 1.5 hours at room temperature, 3x 5 minutes washes, development with chemiluminescence ECL reagent (Perkin Elmer Life Science) and imaged with ImageQuant LAS 4000 (GE Healthcare). For 2D gel electrophoresis, PNGase F treated and untreated rLILRA3 proteins were precipitated with 20% acetone for 1 hour at -20^{o}C. The precipitated proteins were air dried for 10 minutes and rehydrated overnight at room temperature with IPG buffer (8 M urea, 2% (w/v) CHAPS, 10 mM DTT). The next day, 2% ampholyte was added to the rehydrated mix. Isoelectric focusing of the denatured samples was determined by running a 13 cm pH 3-10 Immobiline dry strip (GE healthcare) for a total of 9350 V. After focusing, the strips were equilibrated in 50 mM Tris pH 6.8, 6 M urea, 30% glycerol, and 2% SDS containing 2% DTT for 10 minutes. The reduced proteins were alkylated by incubation in the same buffer containing 2.5% iodoacetamide and electrophoretic separated by layering the strips onto 10% polyacrylamide gels and resolved proteins visualised by silver staining.

Identification of glycosylation sites on the recombinant mammalian LILRA3 by Nano Liquid Chromatography tandem Mass Spectrometry (Nano LC-MS/MS). In brief, 10µg of purified rLILRA3-His from 293T cells was deglycosylated, run under reducing conditions in 10% SDS PAGE and silver stained. Specific bands were then excised, reduced, alkylated with Iodoacetamide (IA) and dehydrated with acetonitrile (ACN). In-gel proteins were digested with 2 ng/µL Trypsin, 6 ng/µL Chymotrypsin, or 6 ng/µL Glu-C. Treated gel bands were incubated in 1% Formic acid (FA) and 3x 100 µL ACN at room temperature. Pooled supernatants from each digest were dried. The dried residues were resuspended in 15µL of 0.05% heptafluorobutyric anhydride and 1% FA and injected into fritless Nano column (75µm x 10cm) of Ultimate 3000 HPLC and autosampler system (Dionex, Amsterdam, Netherlands). Peptides were then eluted using a linear gradient from mobile phase A (0.1% FA in H_2O) to mobile phase B (0.1% FA in 80% ACN) over 35 minutes at a flow rate of 0.3µl/min. Positive ions of tryptic digests were generated by electrospray and a survey scan m/z 350-1750 were acquired in the FT ICR cell of a LTQ-FT Ultra mass analyser (Thermo Electron, Bremen, Germany), and chymotrypsin and Glu-C digests in an Orbitrap mass analyser (Thermo Electron, Bremen, Germany). Peak lists of MS/MS data were generated using Mascot Daemon/extract_msn (Matrix Science, London, England, Thermo) and were interrogated using Mascot version 2.1 (http://www.matrixscience.com) and searched against *Homo sapiens* proteins in the Swissprot protein database (version 80). Precursor tolerances were 4.0 ppm and product ion tolerances were ± 0.4 Da. Modifications accounted for were Acrylamide (C), Carbamidomethyl (C), Deamidation (NQ), and Oxidation (M), with maximum 1 missed cleavage permitted. Enzyme specificity was Trypsin and Semi-trypsin for tryptic digests, V8-DE and no enzyme for Glu-C digests, and Chymotrypsin and no enzyme for chymotryptic digest. Acceptable cut-off scores for individual MS/MS spectra were set to 20. Comparisons of experimental and theoretical tandem mass spectra were automatically performed by Mascot and verified manually. PNGase F treated and non-treated *E. coli* produced rLILRA3 and PNGase F non-treated 293T rLILRA3-His proteins were used as negative controls.

Prediction of N-glycosylation sites in LILRA3. N-glycosylation analysis tool NetNGlyc-1.0, www.cbs.dtu.dk/services/NetNGlyc-1.0, retrieved 17th April 2013 (12), set at a threshold of 0.25-0.5 was used to predict N-linked glycosylation sites in LILRA3.

Quantitative assay for rLILRA3-APtag-His binding to potential ligand(s) on cell surface: To assay for rLILRA3-APtag-His binding, over 25 cell lines from different lineage and peripheral blood leukocyte subsets were initially screened using 100nM of purified protein or control rAP-His. We consistently found specific high affinity binding to U937 cells and peripheral blood monocytes. The U937 cells were used for subsequent kinetic studies, competition experiments and *in situ* staining. In brief, cell lines were cultured in their suitable media containing 10% FBS and primary mononuclear leukocytes were purified by density gradient centrifugation followed by negative selection of monocytes, T cells, B cells and NK cells using magnetic beads (Miltenyi Biotech, Germany) (6). Primary polymorphonuclear cells (>80% neutrophils) were enriched from whole blood by 4.5% dextran in PBS precipitation (Sigma) followed by density gradient centrifugation (13). Cells were washed twice with phosphate-buffered saline (PBS) and once with HBHA buffer (Hank's balanced salt solution (Sigma) containing 0.5mg/mL BSA, 0.1% NaN_3, 20 mM HEPES, pH 7.0) and transferred to 1.5 ml eppendorf tubes at 5x10^{6}/ml of HBHA containing 100nM of rLILRA3-APtag-His or rAPtag-His control. Cells were incubated for 90 minutes at room temperature followed by four washes with 1.5 ml cold HBHA and

centrifugation at 200g, 4°C for 5 minutes and aspiration of supernatant. Cell pellets were lysed with 400 µl of 1% Triton X-100 in 10 mM Tris-HCl, pH 8.5. Lysates were then vortexed vigorously, the nuclei spun out and soluble lysates collected. After heat inactivation of endogenous phosphatases at ~65ºC for 15 minutes, the soluble lysates were assayed in duplicate for alkaline phosphatase activity as described (11).

For competition assays, $5x10^6$ U937 cells in 1 ml of HBHA were pre-incubated with increasing concentrations (0-300nM) of untagged purified recombinant LILRA3 proteins for 1 hour at room temperature. Cells were spun at 200 g for 5 minutes, unbound protein aspirated and cells washed 1x with cold HBHA. Each cell pellet was then resuspended in 1 ml of HBHA and binding to optimal concentration of rLILRA3-APtag-His (30nM) performed as described above. To determine if glycosylation contributes for ligand binding, U937 cells were pre-incubated with 0.1-0.2M β-lactose or control sucrose or NaCl (Sigma) for 1 hour at 37°C followed by a brief wash with cold HBHA and binding to 30nM rLILRA3-APtag-His or rAPtag-His control performed as described (14,15).

In-situ staining of U937 cell with rLILRA3-APtag-His: U937 cells were washed twice with PBS and once with HBHA. Aliquots of $3x10^6$ cells in 300 µl of HBHA were then dispensed into 1.5 ml eppendorf tubes and incubated with 100 nM of purified rLILRA3-APtag-His or rAPtag-His control proteins in HBHA for 90 minutes at room temperature. Following this, rLILRA3-APtag-His and rAPtag-His control treated cells were washed four times with 1.5 ml cold HBHA buffer with gentle vortex and centrifugation at 200g, 4°C for 5 minutes and resuspended in HBHA at $5x10^4$/ml. 200 µl ($1x10^4$) cells from each treatment were then cytospun at 800 rpm for 5 min onto silanized Superfrost® glass slides, fixed in 60% acetone, 3% formaldehyde, 20 mM HEPES for 30 seconds and washed twice in 150 mM NaCl, 20 mM HEPES. Endogenous phosphatases were inactivated by heating slides in 150 mM NaCl, 20 mM HEPES at 65ºC for 10 minutes. This was followed by rinsing of slides with 100 mM Tris-HCl (pH 9.5), 100 mM NaCl, 5 mM $MgCl_2$ and incubation for 15 minutes with alkaline phosphatase substrate containing 10 mM L-homoarginine, 0.17 mg/mL BCIP and 0.33 mg/mL NBT in the same buffer (BCIP/NBT Substrate Kit IV, Vector Laboratories, Burlingame, CA).

Inhibition of LPS-induced monocyte activation by recombinant LILRA3: PBMC from 3 healthy donors were seeded in duplicate in 96-well flat bottom plates at a concentration of $4x10^5$ monocytes /well in 200 µl of RPMI 1640 containing 10% foetal calf serum. Cells were treated with or without 100 ng/ml LPS and in the presence of 0-280 nM of purified recombinant LILRA3 produced in 293T cells or *E. coli* for a dose dependent study. PBMC from further 5 donors were used for repeat studies using optimal concentration of rLILRA3 (70nM) and 100ng/ml LPS. Culture supernatants were collected 24 hours post treatment and levels of secreted TNF-α measured by sandwich ELISA according the manufacturer's instructions (DuoSet, R&D Systems).

RESULTS

High quality, full length recombinant LILRA3 was successfully produced in mammalian cells, E. coli and yeast: Stable transfected 293T cell lines constitutively secreted rLILRA3 with or without APtag-His proteins to culture supernatants. These were purified by cobalt column affinity chromatography to 95-98% purity (Fig 1A and C). Similarly, 85-90% pure, full length rLILRA3 was produced in methanol-induced yeast culture supernatants (data not shown) and from inclusion bodies of transformed *E. coli* (Fig 1E) using one step cobalt column affinity chromatography. Most of the latter protein remained soluble during sequential dialysis and refolding. A typical yield of purified rLILRA3-APtag-His and rLILRA3-His from 1 litre of 293T culture supernatant was 0.75 and 0.4 mg respectively. Similarly, the amount of rLILRA3 produced from 1 litre of yeast culture was modest 0.2 mg. In contrast, up to 15 mg of correctly refolded rLILRA3 protein was purified from a litre of IPTG-induced *E. coli* culture. The apparent molecular weight of rLILRA3 from 293T cells with (Fig 1A, B) or without (Fig 1C, D) rAPtag-His, rLILRA3 from *E. coli* (Fig 1E, F) and rLILRA3 from yeast (data not shown) on SDS-PAGE under reducing conditions were ~130, 70, 50, 65+ kDa respectively. The sizes of the rLILRA3 proteins produced in the 293T cells and yeast were substantially larger than their respective calculated mass of 110 kDa for rLILRA3-APtag-His and 46.61 kDa for the rLILRA3s without tag whereas the size of the rLILRA3 produced in *E. coli* was, similar to the calculated mass of 52.36 kDa, suggesting significant posttranslational modification in recombinant proteins produced by the mammalian and yeast cells. Interestingly, under non-reducing conditions rLILRA3 proteins produced in all systems exist as both monomeric and dimeric forms (Fig 1).

This is not surprising as LILRA3 contains 12 cysteine residues that potentially can form homodimers through multiple disulphide bonds.

The increase in the molecular mass of LILRA3 produced in mammalian and yeast expression systems is due to extensive glycosylation: PNGase F cleaves between N-Acetylglucosamine (GlcNAc) and asparagine (Asn) residues on N-linked high mannose glycans, hybrid glycans, and complex glycans (16). Treatment of recombinant LILRA3 produced in 293T cells and *P. pastoris* with this enzyme reduced their molecular mass to a size similar to the non-glycosylated rLILRA3 produced in *E. coli*, (Fig 2A). This strongly indicates that carbohydrates added to rLILRA3 during post-translational modifications are responsible for the marked increase in mass by more than 15kDa (Fig 2A). As expected, the size of native LILRA3 in primary macrophages was similar to the recombinant LILRA3 produced in 293T cells but larger than the protein produced in *E. coli* (Fig 2A). However, the protein produced in yeast was significantly larger than the native LILRA3 (Fig 2A). This suggests that different expression systems produce highly varied rLILRA3 proteins that may potentially alter LILRA3 characteristics such as its ability to bind its potential ligands and ability to modulate cell functions *in vitro*. As rLILRA3 produced in *E. coli* lacks post-translational modifications while rLILRA3 produced in the lower eukaryote (*P. pastoris)* is possibly hypermannosylated, these recombinant proteins are likely to be functionally inferior to rLILRA3 produced in the higher eukaryotic 293T cells with complex N-glycosylation similar to the native protein.

Glycosylation contributes to the properties of LLRA3: The glycosylated rLILRA3 protein was focused on a spectrum of pH ranging from 6 to 9 with the majority focusing at around 7 despite having the same molecular weight (Fig 2B, upper panel). Treatment with PNGase F reduced the wide pI spectra of the untreated protein to a single focusing at pI 7 (Fig 2B, lower panel). This suggests that the addition of highly charged N-glycan sugar moieties led to the alteration in the charge of the unprocessed protein that have a calculated pI of 8.43. The wide range of isoelectric focusing found on the glycosylated recombinant LILRA3 from 293T cells (Fig 2B, upper panel) indicates the presence of a mixture of proteins with varying degree of glycosylation.

Identification of N-glycosylation sites to the predicted canonical N-glycans in LILRA3: N-glycosylation analysis tool NetNGlyc-1.0 predicted 5 N-linked glycosylation sites in LILRA3 at N_{140}, N_{281}, N_{302}, N_{341} and N_{431} (Supp. Fig 2). Sites at N_{140}, N_{281}, N_{302}, N_{341} were predicted with analysis threshold of 0.5 while N_{431} was predicted at a lower threshold value of 0.25 (Supp. Fig. 2). Experimentally, PNGase F treated recombinant LILRA3 from 293T cells was digested with trypsin, chymotrypsin or Glu-C and peptides analysed using tandem Nano LC-MS/MS (Fig 3). Digestion with Glu-C identified 3 deamidated residues at N_{140} (Fig 3A), N_{281} (Fig 3A) and N_{431} (Fig 3A); trypsin digest identified 2 deamidated asparagine residues at N_{281} (Fig 3B) and N_{431} (Fig 3B) and chymotrypsin identified 2 deamidated residues at N_{281} (Fig 3C) and N_{341} (Fig 3C). It is noteworthy that some sites were identified by more than one enzyme (Fig 3). Deamidation of the predicted N_{302} site was not found in the initial experiment (Fig 3). In two subsequent experiments, in addition to confirming the findings on the Glu-C and chymotrypsin digested peptides, digestion of peptides with trypsin detected all the predicted sites including N_{302} (Fig 4) (Table 1). Importantly, we found <2% (1 in 54 occurrences) of deamidation of any sites in *E. coli* produced rLILRA3 control with or without PNGase F treatment followed by peptide digest (Table 1) (Supp Fig 3). As expected, rLILRA3 produced in the mammalian 293T cells not treated with PNGase F did not generate matching peptides to the PNGase F treated protein due to the presence of the large N-glycans (Table 1).

Screening for LILRA3 binding on cell surface using placental alkaline phosphatase tagged recombinant LILRA3: Surface binding of rLILRA3-APtag-His to primary leukocytes subsets and cell lines was screened, using a simple and highly sensitive method (11) and found U937 monocytic cell line showed the highest binding to rLILRA3-APtag-His with ~80μU of specific alkaline phosphatase activity followed by Raji B cells (~50μU), PBMC (~37μU) and HL-60 myeloid cells (~14μU) (Fig 5A). There was little or no binding of rLILRA3-APtag to THP-1 cells, Jurkat T cell and NK-92 cells (Fig 5A). Among the primary leukocytes, purified primary monocytes showed the strongest binding to rLILRA3-APtag-His with net alkaline phosphatase activity of ~90μU as compared to PMN that showed moderate binding (~24μU). In contrast T, B and NK cells showed minimal binding to rLILRA3-APtag-His (Fig 5B). None of the 20 cell lines of epithelial or mesenchymal lineage tested showed significant binding to rLILRA3-APtag-His except for a neuronal cell line SKNSH that showed substantial binding (data not shown). *In situ* staining of U937 cytospins using rLILRA3-APtag-His or rAPtag-His control showed cell surface staining only on cells incubated with

rLILRA3-APtag-His but not rAPtag-His (Fig 5C), suggesting expression of LILRA3 ligand(s) on the surface of these cells. Binding of rLILRA3-APtag-His to U937 cells was competitively blocked by pre-incubation of cells with untagged rLILRA3 but not buffer control in a dose dependent manner (Fig 5D), confirming specific binding. Interestingly, pre-incubation of U937 cells with 10 fold excess of recombinant LILRA3 produced in the yeast poorly blocked rLILRA3-APtag-His binding by only 20% (data not shown) and *E. coli* produced rLILRA3 totally failed to inhibit binding as contrasted to >90% blocking by mammalian produced untagged protein (Fig 5E). These results suggest that optimal post-translational modification in the mammalian expression system is required for binding of LILRA3 to its potential cell surface ligand(s).

LILRA3 glycosylation contributes to effective ligand binding: Given glycosylation was the major post-translational modification that altered the physical properties of the mammalian rLILRA3 (Figs 2, 3, 4), the effects of these modifications to its ability to bind U937 cells were assessed by pre-treatment of cells with β-lactose. Pre-incubation of cells with 0.1M or 0.2M β-lactose blocked rLILRA3 binding by an average of 10 ± 0.3% and 40 ± 0.5% respectively (Fig 5F) but not control sucrose or NaCl (Fig 5G), indicating that N-glycosylation partially played a role in its ability to bind ligand(s). These results strongly complement our observation that *E. coli* produced non-glycosylated rLILRA3 (Fig 5E) or yeast produced "inappropriately" glycosylated rLILRA3 (data not shown) do not competitively block binding.

Mammalian but not E. coli derived recombinant LILRA3 down-regulates LPS-mediated TNFα production in PBMC. Incubation of freshly isolated normal PBMCs with 100pg/ml of LPS *in vitro* induced high levels of TNFα production ranging between 5500-9000pg/ml (Fig 6). Simultaneous treatment of cells with 17-280nM of recombinant mammalian LILRA3 significantly abrogated LPS-induced TNF*α* production in a dose dependent manner (Fig 6A). Treatment of cells with optimal dose of rLILRA3 (consistently suppressed TNF production by up to 60% in a dose dependent manner (Fig 6A) in multiple donors (Fig 6B). However, equivalent amounts of recombinant LILRA3 produced in *E. coli* did not suppress LPS-induced TNF production in all donors (data not shown). This is consistent with the ability of mammalian derived rLILRA3 but not *E. coli* to bind to the surface of PBMCs and modulate function.

DISCUSSION

In this report we have successfully generated recombinant LILRA3 in *E. coli*, yeast and 293T cells and assessed their yield, properties and biological functions. We found that *P. pastoris* and 293T cells but not *E. coli* produced substantially larger size rLILRA3 than the calculated mass of the unmodified protein, indicating marked post-translational modifications (Figs 1, 2). Treatment with PNGase F reduced yeast and mammalian produced proteins to a size equivalent to the expected unmodified protein, suggesting both proteins underwent N-glycan modifications but with varied outcomes. N-glycan modification in all eukaryotic cells starts as a common $Man_8GlcNAc_2$ precursor, produced after some initial processing, but in higher eukaryotes the α-1-2-mannose residues are removed and complex N-linked glycosylated proteins are formed (17). By contrast, $Man_8GlcNAc_2$ in yeast are further elongated by several mannosyltransferases resulting in the formation of large hyperglycosylated or hypermannosylated products of native (18) or complex foreign proteins (19). Hence the significantly larger molecular mass of rLILRA3 produced in *P. pastoris* as compared to native LILRA3 is likely due to hyperglycosylation or hypermannosylation (Fig 2A), whereas the mammalian produced protein may have undergone appropriate glycosylation and is thus structurally and functionally closer to native LILRA3. Consistent with the latter, we showed that native LILRA3 from primary macrophages was the same size as recombine protein produced in mammalian cells but not yeast or *E. coli* (Fig 2).

LILRA3 produced in the mammalian system showed multiple isoelectric focusing however upon treatment with PNGase F reduced to a single pI (Fig 2), indicating changes in the biochemical property of this protein was due to addition of highly charged N-glycans. This is similar to previous data showing glycosylation significantly altering pI of other similar glycoproteins (20,21). Moreover, glycosylation can provide conformational and structural stability (22,23), may facilitate correct folding (23,24) and importantly modulate ligand binding and functions (20,25,26). We find rLILRA3 in its non-glycosylated form required extensive refolding steps, was highly susceptible to aggregation/oxidation and was non-functional, despite being high purity and high yield (up to 15mg/L). Similarly, production of hyperglycosylated rLILRA3 in yeast may have altered its biochemical property that contributed to its low production efficiency (0.25 mg/L) and poor function.

By contrast, optimal glycosylation of the mammalian produced rLILRA3 protein may have facilitated to its efficient folding, sufficient production (0.4-0.8 mg/L), high stability and excellent biological functions (Figs 5,6). Our successful blocking experiment using β-lactose further enforces the suggestion that ligand binding and possibly suppression of TNFα production was at least partially dependent on optimal glycosylation (Fig 5). We therefore, were compelled to identify the specific N-glycosylation sites as a prelude for future functional characterisation using site target mutagenesis.

LILRA3 is predicted to contain 5 N-glycosylation sites onto specific asparagine residues within consensus sequences of N-X-S/T (X is any amino acid other than P) (27). We utilised a combination of electrophoresis and Nano LC-MS/MS and identified all 5 N-glycosylated sites at N_{140}, N_{281}, N_{302}, N_{341} and N_{431}. This is the first study that experimentally mapped specific glycosylation sites on any LILR protein. Recently it has been reported that deglycosylation with PNGase F can lead to false positive assignments of N-glycosylation sites (28). False positive deamidation commonly occur in small and hydrophilic amino acids such as glycine and serine at position X of the N-X-S/T/C consensus sequence (16). Although LILRA3 does not contain such consensus sequences, we performed stringent control experiments using *E. coli* produced rLILRA3 with or without PNGase treatment and PNGase-untreated mammalian rLILRA3-His. As expected *E. coli* produced rLILRA3 with or without PNGase F treatment or untreated mammalian derived rLILRA3 showed negligible spontaneous deamidation with false discovery rate of <2%, indicating specificity. Initially, three different peptide digestion enzymes were required to map 4 of the 5 sites in which N_{281} was detected with all three enzymes, N_{140} and N_{341} were apparent with Glu-C or chymotrypsin digest and N_{431} was detected in both trypsin and Glu-C digested peptides (Fig 3). This is in agreement with reports showing bottom-up proteomics would generate different peptide coverage depending on the choice of enzyme (29,30). Interestingly, in subsequent experiments digestion with trypsin alone was sufficient for full peptide coverage and detected all 5 N-glycosylation sites including N_{302} (Fig 4). N_{302} site could not be initially detected, possibly due to inability to generate enough peptides for a full coverage as a result of the use of insufficient amount of rLILRA3.

It is noteworthy that LILRA3 is also predicted to have up to 8 potential O-linked glycosylated sites (NetOGlyc 4.0 analysis tool, http://www.cbs.dtu.dk/services/NetOGlyc) (31) that may contribute to its structure and/or functions requiring future investigation.

Our data demonstrate that production of optimally glycosylated LILRA3 in the mammalian system was necessary for its high affinity binding to its potential ligand(s) (Fig 5). However, most studies of the LILR family to date did not consider the likely importance of appropriate glycosylation to high affinity ligand binding and function. To date LILRB1, LILRB2, LILRA1 and LILRA3 have been shown to bind various classical and non-classical MHC-class I molecules (32-34) and a viral homolog UL-18 (32). However, these are mostly low affinity and interactions with varied dissociation constants ranging from 2-12 μM (35,36) and they lack robust functional data. This is possibly due to the use of truncated extracellular domains of LILRs produced in *E. coli* that are inefficiently folded and not appropriately post-translationally modified. Alternatively, LILRs may have hierarchical tissue-specific interaction to multiple ligands *in vivo* or MHC-class I molecules might be co-ligands, an issue grossly overlooked so far. Indeed, recently, several LILRs were also shown to functionally bind non-MHC class I molecules with much higher affinity than binding to MHC-class I. These include binding of Nogo-66 (37) and ANGPTL5 (38) to LILRB2 and binding of BST-2 to LILRA4 (39).

In this study we presented a simple robust approach for rapid high throughput screening and *in-situ* localisation of LILRA3 cell surface binding. The additional advantages for the use of mammalian LILRA3 protein tagged to placental alkaline phosphatase include the high specific activity of the mammalian enzyme, its high stability, including stability to heat of the placental isoenzyme, the availability of isoenzyme-specific inhibitors, availability of a variety of indicator substrates for alkaline phosphatase (11) and availability of high quality anti-placental alkaline phosphatase antibodies (GeneHunter, USA). This provided us with key tools for future simultaneous identification LILR ligands and co-ligands using selected LILRA3 binding cells. Moreover, the rapid screening of rLILRA3-APtag-His binding proteins allowed us to objectively select suitable cells for our functional studies.

We showed LILRA3 preferably binds on the surface of monocytes and the monocytic cell line U937. This suggests that LILRA3 may predominantly regulate mono-myeloid cells. We showed for the first time that LILRA3 abrogated LPS-mediated TNFα

production suggesting direct inhibitory effect transduced through yet unknown surface ligand(s). LILRA3 may also exert its effects by competitively antagonising closely related cell surface activating LILRs. A recent study showed LILRA3 and LILRA1 (88% homology) may share common MHC-class I ligand(s) (34), although the functional consequence of this needs to be defined. We propose LILRA3 is a novel anti-inflammatory protein that directly suppress excessive leukocyte activation and/or by acting as a soluble antagonist to activating LILRs, akin to the soluble TNFα receptor and IL-6R (40,41). This is consistent with our recent finding of abundant presence of LILRA3 protein in sera of health individuals and its significant up-regulation by the anti-inflammatory cytokine IL-10 (6). This is further supported by recent reports showing association between lack of LILRA3 with increased incidence of multiple sclerosis (8,9) and Sjogren's syndrome (10), diseases characterised by chronic inflammation. Interestingly, we found significant increase in LILRA3 in sera of patients with active RA (6) together with increased expression of activating and inhibitory LILRs in synovial tissue (7). This may suggest an increase in LILRA3 to oppose the ongoing inflammation or a proportion of the high level LILRA3 in patient sera might be aberrantly glycosylated leading to poor function. Abnormal ligand binding and functions due to altered glycosylation of endogenous proteins such as IgG have been reported in rheumatoid arthritis (42,43). Whether LILRA3 which has structural similarities to IgG also display abnormal glycan modifications that alter its function requires further investigation.

REFERENCES

1. Brown, D., Trowsdale, J., and Allen, R. (2004) The LILR family: modulators of innate and adaptive immune pathways in health and disease. *Tissue Antigens* **64**, 215-225
2. Nakajima, H., Samaridis, J., Angman, L., and Colonna, M. (1999) Human myeloid cells express an activating ILT receptor (ILT1) that associates with Fc receptor gamma-chain. *J Immunol* **162**, 5-8
3. Cosman, D., Fanger, N., Borges, L., Kubin, M., Chin, W., Peterson, L., and Hsu, M. L. (1997) A novel immunoglobulin superfamily receptor for cellular and viral MHC class I molecules. *Immunity* **7**, 273-282
4. Torkar, M., Haude, A., Milne, S., Beck, S., Trowsdale, J., and Wilson, M. J. (2000) Arrangement of the ILT gene cluster: a common null allele of the ILT6 gene results from a 6.7-kbp deletion. *Eur J Immunol* **30**, 3655-3662
5. Wilson, M. J., Torkar, M., Haude, A., Milne, S., Jones, T., Sheer, D., Beck, S., and Trowsdale, J. (2000) Plasticity in the organization and sequences of human KIR/ILT gene families. *Proc Natl Acad Sci U S A* **97**, 4778-4783
6. An, H., Chandra, V., Piraino, B., Borges, L., Geczy, C., McNeil, H. P., Bryant, K., and Tedla, N. (2010) Soluble LILRA3, a potential natural antiinflammatory protein, is increased in patients with rheumatoid arthritis and is tightly regulated by interleukin 10, tumor necrosis factor-alpha, and interferon-gamma. *J Rheumatol* **37**, 1596-1606
7. Tedla, N., An, H., Borges, L., Vollmer-Conna, U., Bryant, K., Geczy, C., and McNeil, H. P. (2011) Expression of activating and inhibitory leukocyte immunoglobulin-like receptors in rheumatoid synovium: correlations to disease activity. *Tissue Antigens* **77**, 305-316
8. Koch, S., Goedde, R., Nigmatova, V., Epplen, J. T., Muller, N., de Seze, J., Vermersch, P., Momot, T., Schmidt, R. E., and Witte, T. (2005) Association of multiple sclerosis with ILT6 deficiency. *Genes Immun* **6**, 445-447
9. Ordonez, D., Sanchez, A. J., Martinez-Rodriguez, J. E., Cisneros, E., Ramil, E., Romo, N., Moraru, M., Munteis, E., Lopez-Botet, M., Roquer, J., Garcia-Merino, A., and Vilches, C. (2009) Multiple sclerosis associates with LILRA3 deletion in Spanish patients. *Genes Immun*
10. Kabalak, G., Dobberstein, S. B., Matthias, T., Reuter, S., The, Y. H., Dorner, T., Schmidt, R. E., and Witte, T. (2009) Association of immunoglobulin-like transcript 6 deficiency with Sjogren's syndrome. *Arthritis Rheum* **60**, 2923-2925
11. Flanagan, J. G., and Leder, P. (1990) The kit ligand: a cell surface molecule altered in steel mutant fibroblasts. *Cell* **63**, 185-194
12. Gupta, R., Jung, E., and Brunak, S. (2004) Prediction of N-glycosylation sites in human proteins. *In preparation*
13. Tedla, N., Bandeira-Melo, C., Tassinari, P., Sloane, D. E., Samplaski, M., Cosman, D., Borges, L., Weller, P. F., and Arm, J. P. (2003) Activation of human eosinophils through leukocyte immunoglobulin-like receptor 7. *Proc Natl Acad Sci U S A* **100**, 1174-1179
14. Fermino, M. L., Polli, C. D., Toledo, K. A., Liu, F. T., Hsu, D. K., Roque-Barreira, M. C., Pereira-da-Silva, G., Bernardes, E. S., and Halbwachs-Mecarelli, L. (2011) LPS-induced galectin-3 oligomerization results in enhancement of neutrophil activation. *PloS one* **6**, e26004
15. Stillman, B. N., Hsu, D. K., Pang, M., Brewer, C. F., Johnson, P., Liu, F. T., and Baum, L. G. (2006) Galectin-3 and galectin-1 bind distinct cell surface glycoprotein receptors to induce T cell death. *J Immunol* **176**, 778-789
16. Martinez-Donato, G., Acosta-Rivero, N., Morales-Grillo, J., Musacchio, A., Vina, A., Alvarez, C., Figueroa, N., Guerra, I., Garcia, J., Varas, L., Muzio, V., and Duenas-Carrera, S. (2006) Expression and processing of hepatitis C virus structural proteins in Pichia pastoris yeast. *Biochem Biophys Res Commun* **342**, 625-631

17. Helenius, A., and Aebi, M. (2004) Roles of N-linked glycans in the endoplasmic reticulum. *Annual review of biochemistry* **73**, 1019-1049
18. Vervecken, W., Kaigorodov, V., Callewaert, N., Geysens, S., De Vusser, K., and Contreras, R. (2004) In vivo synthesis of mammalian-like, hybrid-type N-glycans in Pichia pastoris. *Appl Environ Microbiol* **70**, 2639-2646
19. Guo, M., Hang, H., Zhu, T., Zhuang, Y., Chu, J., and Zhang, S. (2008) Effect of glycosylation on biochemical characterization of recombinant phytase expressed in Pichia pastoris. *Enzyme and Microbial Technology* **42**, 340-345
20. Margraf-Schonfeld, S., Bohm, C., and Watzl, C. (2011) Glycosylation affects ligand binding and function of the activating natural killer cell receptor 2B4 (CD244) protein. *J Biol Chem* **286**, 24142-24149
21. Kunicki, T. J., Cheli, Y., Moroi, M., and Furihata, K. (2005) The influence of N-linked glycosylation on the function of platelet glycoprotein VI. *Blood* **106**, 2744-2749
22. Zou, S., Huang, S., Kaleem, I., and Li, C. (2013) N-glycosylation enhances functional and structural stability of recombinant beta-glucuronidase expressed in Pichia pastoris. *Journal of biotechnology* **164**, 75-81
23. Wormald, M. R., and Dwek, R. A. (1999) Glycoproteins: glycan presentation and protein-fold stability. *Structure* **7**, R155-160
24. Shental-Bechor, D., and Levy, Y. (2008) Effect of glycosylation on protein folding: a close look at thermodynamic stabilization. *Proc Natl Acad Sci U S A* **105**, 8256-8261
25. Guseva, N. V., Fullenkamp, C. A., Naumann, P. W., Shey, M. R., Ballas, Z. K., Houtman, J. C., Forbes, C. A., Scalzo, A. A., and Heusel, J. W. (2010) Glycosylation contributes to variability in expression of murine cytomegalovirus m157 and enhances stability of interaction with the NK-cell receptor Ly49H. *Eur J Immunol* **40**, 2618-2631
26. Uchibori-Iwaki, H., Yoneda, A., Oda-Tamai, S., Kato, S., Akamatsu, N., Otsuka, M., Murase, K., Kojima, K., Suzuki, R., Maeya, Y., Tanabe, M., and Ogawa, H. (2000) The changes in glycosylation after partial hepatectomy enhance collagen binding of vitronectin in plasma. *Glycobiology* **10**, 865-874
27. Geetha-Habib, M., Park, H. R., and Lennarz, W. J. (1990) In vivo N-glycosylation and fate of Asn-X-Ser/Thr tripeptides. *J Biol Chem* **265**, 13655-13660
28. Palmisano, G., Melo-Braga, M. N., Engholm-Keller, K., Parker, B. L., and Larsen, M. R. (2012) Chemical deamidation: a common pitfall in large-scale N-linked glycoproteomic mass spectrometry-based analyses. *J Proteome Res* **11**, 1949-1957
29. Kalli, A., and Hakansson, K. (2008) Comparison of the electron capture dissociation fragmentation behavior of doubly and triply protonated peptides from trypsin, Glu-C, and chymotrypsin digestion. *J Proteome Res* **7**, 2834-2844
30. Zielinska, D. F., Gnad, F., Wisniewski, J. R., and Mann, M. (2010) Precision mapping of an in vivo N-glycoproteome reveals rigid topological and sequence constraints. *Cell* **141**, 897-907
31. Steentoft, C., Vakhrushev, S. Y., Joshi, H. J., Kong, Y., Vester-Christensen, M. B., Schjoldager, K. T., Lavrsen, K., Dabelsteen, S., Pedersen, N. B., Marcos-Silva, L., Gupta, R., Bennett, E. P., Mandel, U., Brunak, S., Wandall, H. H., Levery, S. B., and Clausen, H. (2013) Precision mapping of the human O-GalNAc glycoproteome through SimpleCell technology. *EMBO J* **32**, 1478-1488
32. Vitale, M., Castriconi, R., Parolini, S., Pende, D., Hsu, M. L., Moretta, L., Cosman, D., and Moretta, A. (1999) The leukocyte Ig-like receptor (LIR)-1 for the cytomegalovirus UL18 protein displays a broad specificity for different HLA class I alleles: analysis of LIR-1 + NK cell clones. *Int Immunol* **11**, 29-35

33. Chapman, T. L., Heikeman, A. P., and Bjorkman, P. J. (1999) The inhibitory receptor LIR-1 uses a common binding interaction to recognize class I MHC molecules and the viral homolog UL18. *Immunity* **11**, 603-613
34. Jones, D. C., Kosmoliaptsis, V., Apps, R., Lapaque, N., Smith, I., Kono, A., Chang, C., Boyle, L. H., Taylor, C. J., Trowsdale, J., and Allen, R. L. (2011) HLA class I allelic sequence and conformation regulate leukocyte Ig-like receptor binding. *J Immunol* **186**, 2990-2997
35. Shiroishi, M., Kajikawa, M., Kuroki, K., Ose, T., Kohda, D., and Maenaka, K. (2006) Crystal structure of the human monocyte-activating receptor, "Group 2" leukocyte Ig-like receptor A5 (LILRA5/LIR9/ILT11). *J Biol Chem* **281**, 19536-19544
36. Chapman, T. L., Heikema, A. P., West, A. P., Jr., and Bjorkman, P. J. (2000) Crystal structure and ligand binding properties of the D1D2 region of the inhibitory receptor LIR-1 (ILT2). *Immunity* **13**, 727-736
37. Atwal, J. K., Pinkston-Gosse, J., Syken, J., Stawicki, S., Wu, Y., Shatz, C., and Tessier-Lavigne, M. (2008) PirB is a Functional Receptor for Myelin Inhibitors of Axonal Regeneration. *Science* **322**, 967-970
38. Zheng, J., Umikawa, M., Cui, C., Li, J., Chen, X., Zhang, C., Huynh, H., Kang, X., Silvany, R., Wan, X., Ye, J., Canto, A. P., Chen, S. H., Wang, H. Y., Ward, E. S., and Zhang, C. C. (2012) Inhibitory receptors bind ANGPTLs and support blood stem cells and leukaemia development. *Nature* **485**, 656-660
39. Cao, W., Bover, L., Cho, M., Wen, X., Hanabuchi, S., Bao, M., Rosen, D. B., Wang, Y. H., Shaw, J. L., Du, Q., Li, C., Arai, N., Yao, Z., Lanier, L. L., and Liu, Y. J. (2009) Regulation of TLR7/9 responses in plasmacytoid dendritic cells by BST2 and ILT7 receptor interaction. *J Exp Med* **206**, 1603-1614
40. Jones, S. A., Horiuchi, S., Topley, N., Yamamoto, N., and Fuller, G. M. (2001) The soluble interleukin 6 receptor: mechanisms of production and implications in disease. *FASEB J* **15**, 43-58
41. Arck, P. C., Troutt, A. B., and Clark, D. A. (1997) Soluble receptors neutralizing TNF-alpha and IL-1 block stress-triggered murine abortion. *American journal of reproductive immunology* **37**, 262-266
42. Parekh, R. B., Dwek, R. A., Sutton, B. J., Fernandes, D. L., Leung, A., Stanworth, D., Rademacher, T. W., Mizuochi, T., Taniguchi, T., Matsuta, K., and et al. (1985) Association of rheumatoid arthritis and primary osteoarthritis with changes in the glycosylation pattern of total serum IgG. *Nature* **316**, 452-457
43. Alavi, A., Arden, N., Spector, T. D., and Axford, J. S. (2000) Immunoglobulin G glycosylation and clinical outcome in rheumatoid arthritis during pregnancy. *J Rheumatol* **27**, 1379-1385

FIGURE LEGENDS

FIGURE 1: Representative silver staining and Western blotting of rLILRA3 from 293T cells and *E. coli* showing high quality protein production. A) Silver staining of culture supernatant from rLILRA3-APtag-His overexpressing 293T cells showing abundant expression of protein (lane 1) and sequential fractions of cobalt column purified proteins from the same culture supernatant eluted using 50 mM imidazole (lanes 2, 3) and 150 mM imidazole (lane 4) showing highly purified protein. **B)** Western blotting of cobalt column purified rLILRA3-APtag-His proteins using anti-AP Ab showing a single band under reduced condition with DTT (lane 1) but some dimerization under non-reduced conditions (lane 2). **C)** Silver staining of culture supernatant from rLILRA3-His overexpressing 293T cells showing abundant expression of protein (lane 1), unbound protein after cobalt column affinity binding (lane 2) and sequential fractions of cobalt column purified proteins from the same culture supernatant eluted using 50 mM imidazole (lane 3) and 150 mM imidazole (lane 4) showing highly purified protein. **D)** Western blotting of cobalt column purified rLILRA3-His proteins using anti-LILRA3 mAb showing a single band under reduced condition (lane 1) but some dimerization under non-reduced conditions (lane 2). **E)** Coomassie staining of rLILRA3 in inclusion body of *E. coli* after solubilisation with 8M (lane 1) and after purification with cobalt affinity column (lane 2), followed by dialysis in buffer B (lane 3) and refolding in buffer A (lane 4). **F)** Western blotting of refolded rLILRA3 from *E. coli* using anti-LILRA3 mAb showing a single band under reduced condition (lane 1) and some dimerization under non-reduced conditions (lane 2).

FIGURE 2: N-glycosylation altered the molecular mass and the biochemical properties of LILRA3. A) Western blotting of PNGase F treated (P+) and PNGase F untreated (P-) rLILRA3 from 293T cells and *P. pastoris* using anti-LILRA3 mAb showed substantial reduction in molecular mass of both eukaryotic-cell produced recombinant proteins following deglycosylation. Recombinant LILRA3 produced in *E. coli* served as a control for non-glycosylated protein. Non-PNGase F treated LILRA3 from native macrophages of two individual donors are shown as positive references to optimally glycosylated protein. **B)** Silver staining of two dimensional gel of non-deglycosylated purified rLILRA3 from 293T cells showed a spectrum of isoelectric focusing with pI ranging from 6 to 9 (upper panel) but upon deglycosylation using PNGase F, it was reduced to a single focus with a pI of 7 (lower panel).

FIGURE 3: Representative Nano LC-MS/MS of PNGase F deglycosylated-peptide digested mammalian rLILRA3 confirmed 4 predicted N-glycosylation sites. A) In gel peptide digestion of deglycosylated rLILRA3 with Glu-C showed deamidation of asparagine to aspartic acid at N_{140} (i), N_{281} (ii) and N_{431} (iii) indicating N-linked glycosylation of these sites. **B)** Digestion with chymotrypsin showed deamidation at N_{281} (i) and N_{341} (ii), and **(C)** Digestion with trypsin detected N_{281} (i) and N_{431} (ii). It is noteworthy that some sites were detected in peptides digested by more than one enzyme and none of the enzymes provided full peptide coverage. The predicted N_{302} was not detected. The sequence of the peptide, the fragmentation pattern and the detected fragment ions are shown top-right of each panel. *b* ions contain the N-terminal region of the peptide, *y* ions contain the C-terminal region of the peptide. Deamidation of asparagine to aspartic acid is designated as "N" with an underscore.

FIGURE 4: A repeat Nano LC-MS/MS of PNGase F deglycosylated-trypsin digested mammalian rLILRA3 confirmed all 5 predicted N-glycosylation sites. In gel peptide digestion of deglycosylated rLILRA3 with trypsin showed deamidation of asparagine to aspartic acid at $N_{140,}$ (A) N_{281} (B), N_{302} (C), N_{341} (D) and N_{431} (E), indicating N-linked glycosylation of these sites. The sequence of the peptide, the fragmentation pattern and the detected fragment ions are shown top-right of each panel. *b* ions contain the N-terminal region of the peptide, *y* ions contain the C-terminal region of the peptide. Deamidation of asparagine to aspartic acid is designated as "N" with an underscore.

FIGURE 5: High affinity binding of rLILRA3 to the surface of monocytes; partial blocking of binding by β lactose. A) Screening of leukocytic cell lines and PBMC showing strong surface binding of purified rLILRA3-rAPtag-His on the surface of PBMC, U937 monocytic cell line and Raji B cell line. There was minimal binding to rAPtag-His control protein (n=6). **B)** Binding assay using purified primary leukocyte subsets showing significant binding of purified rLILRA3-APtag-His on the surface of monocytes and neutrophils (PMN) but limited binding to T cells, B cells or NK cells (n=3). **C)** Representative *in situ* staining of U937 cells using purified rLILRA3-APtag-His or rAPtag-His alone showed strong surface staining/binding of rLILRA3-APtag-His (left) but not rAPtag-His alone (right) as detected by BCIP/NBT alkaline phosphatase substrate stained in blue and neutral red nuclear counterstain (250x magnification; n=5). **D)** Binding of 30nM of purified rLILRA3-rAPtag-His to U937 cells was

competitively blocked with pre-incubation of cells with untagged rLILRA3 in a dose dependent manner, confirming binding specificity (n=3) (One way Anova, *p<0.05; **p<0.01 as compared to corresponding buffer control). **E)** Binding of 30nM of purified rLILRA3-APtag to U937 cells was blocked by 10 fold excess of untagged purified rLILRA3 from 293T cells but not from *E. coli* recombinant LILRA3 (n=3) (One way Anova, *p<0.05 compared to rLILRA3-APtag alone). **F)** Binding of 30nM of purified rLILRA3-APtag to U937 cells was partially blocked by β lactose in a dose dependent manner, suggesting the sugar moiety components may be required for ligand binding (n=3) (One way Anova, *p<0.05 compared to buffer (PBS) control). **G)** 0.2 M β lactose but not 0.2 M sucrose or 0.2N NaCl in PBS blocked rLILRA3-APtag (30nM) binding to the surface of U937 cells confirming specificity (n=5) (One way Anova, *p<0.05; **p<0.01 compared to PBS (buffer) control).

FIGURE 6: Recombinant LILRA3 produced in 293T cells suppressed LPS-mediated TNFα production by PBMC. A) Simultaneous treatment of PBMC with increasing concentrations of purified rLILRA3 100ng/ml of LPS for 24 hours caused dose dependent suppression of TNFα production. Cells treated with rLILRA3 alone produced minimal TNFα (n=3) (One way ANOVA *p<0.05; **p<0.01 compared to no rLILRA3 control). **B)** Treatment of PBMC from 5 healthy subjects with 100ng/ml LPS and optimal concentration of rLILRA3 (70nM) for 24 hours consistently showed 35-45% suppression of TNFα production. Cells treated with rLILRA3 but not LPS showed minimal TNF production. One way ANOVA *p < 0.05 compared no rLILRA3 control.

TABLE 1: LC-MS/MS summary of N-linked glycosylation sites on PNGase F-treated- trypsin digested recombinant LILRA3 produced in 293T cells showing deamidation of all 5 predicted sites as compared to <2% spontaneous deamidation (false positive) in *E. coli* produced protein. Non-PNGase F treated-trypsin digested recombinant LILRA3 produced in both mammalian cells and *E. coli* were used as relevant negative controls. The peptide fragments containing asparagine (N) were given an ion score and analysed for deamidation. Positive deamidation is designated as "Yes" and no deamidation is designated as "No". If no peptide was detected it is designated as "ND".

	PNGase F treated				*Non-PNGase F treated*			
	293T		*E. coli*		293T		*E. coli*	
N-Site	Ion Score	Deamidation Yes/No	Ion Score	Deamidation Yes/No	Ion Score	Deamidation Yes/No	Ion Score	Deamidation Yes/No
140	51	Yes	66	No	ND	ND	47	No
	25	Yes	68	No			45	No
			80	No				
281	26	Yes	52	No	60	No	41	No
	28	Yes	55	No			85	No
	109	Yes	90	No			34	No
	32	Yes	29	No			30	No
	110	Yes	42	No			65	No
	76	Yes	34	No			23	No
	30	Yes	57	No			32	No
	91	Yes	59	No			39	No
	53	Yes	64	No			78	No
	20	Yes	42	No			51	No
	77	Yes	59	No			26	No
	57	Yes	54	No			58	No
			56	No			29	No
			48	No			71	No
			32	No			43	No
			30	No			73	No
			24	No				
			91	No				
			39	No				
			33	No				
302	49	Yes	44	No	ND	ND	45	No
	95	Yes	81	No			79	No
			55	No				
341	64	Yes	20	No	ND	ND	30	No
	28	Yes	49	No			39	No
	33	Yes	21	No			24	No
	42	Yes	28	No			50	No
	53	Yes	60	No			23	No
	65	Yes	57	No			44	No
	72	Yes	43	No			34	No
	38	Yes	36	No			5	No
	39	Yes	53	No			56	No
			60	No			53	No
			84	No			56	No
			61	No			64	No
			55	No			40	No
			39	No			63	No
			27	No			46	No
			33	No			24	No
							47	No
							56	No
							42	No
							39	No
							71	No
							61	No
							35	No
431	51	No	53	No	31	No	25	No
	54	Yes	31	No			49	No
	38	Yes	36	No			34	No
	52	Yes	30	No			25	No
	31	Yes	23	No			31	No
	30	Yes	38	No			48	No
	22	Yes	43	No			45	No
	29	Yes	49	No			38	No
	21	Yes	30	No			67	No
	44	Yes	29	**Yes**			100	No
			30	No				
			36	No				

FIGURE 1

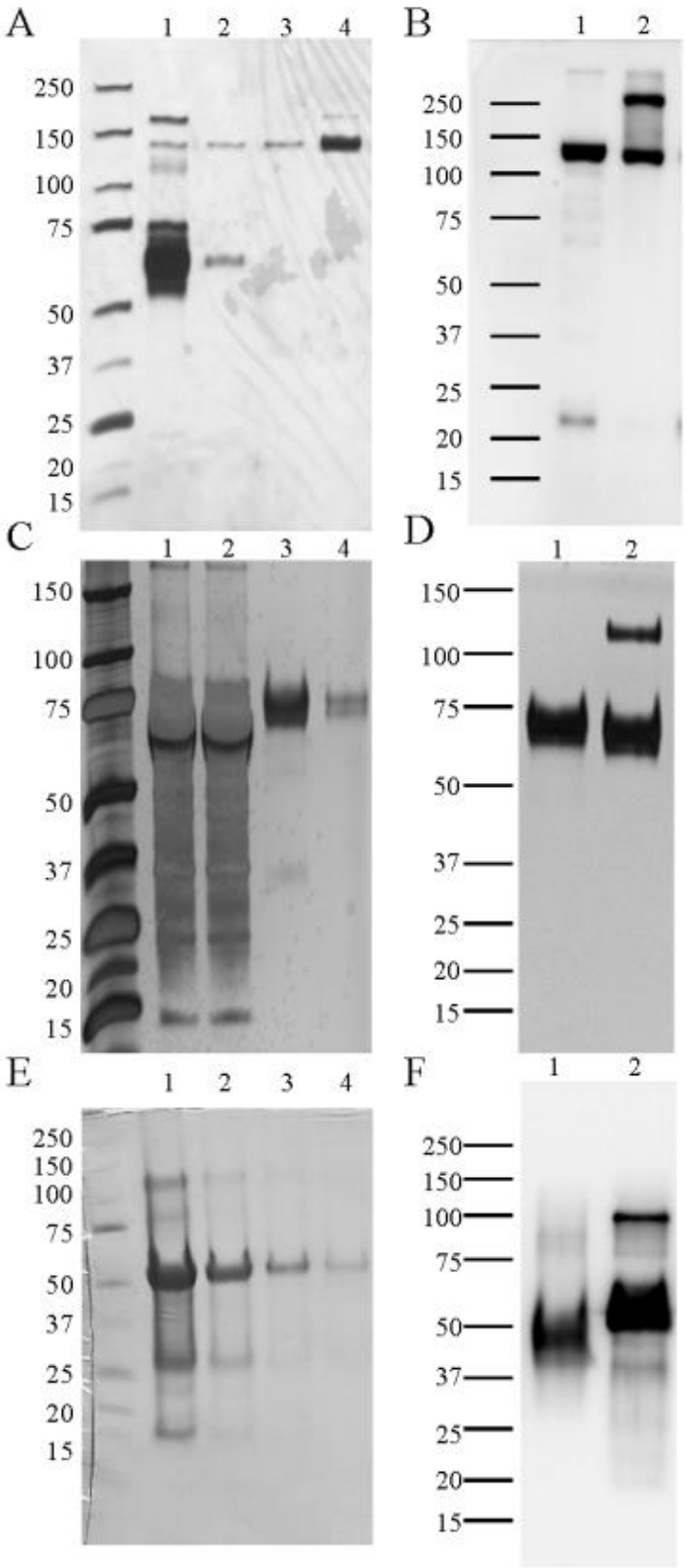

FIGURE 2

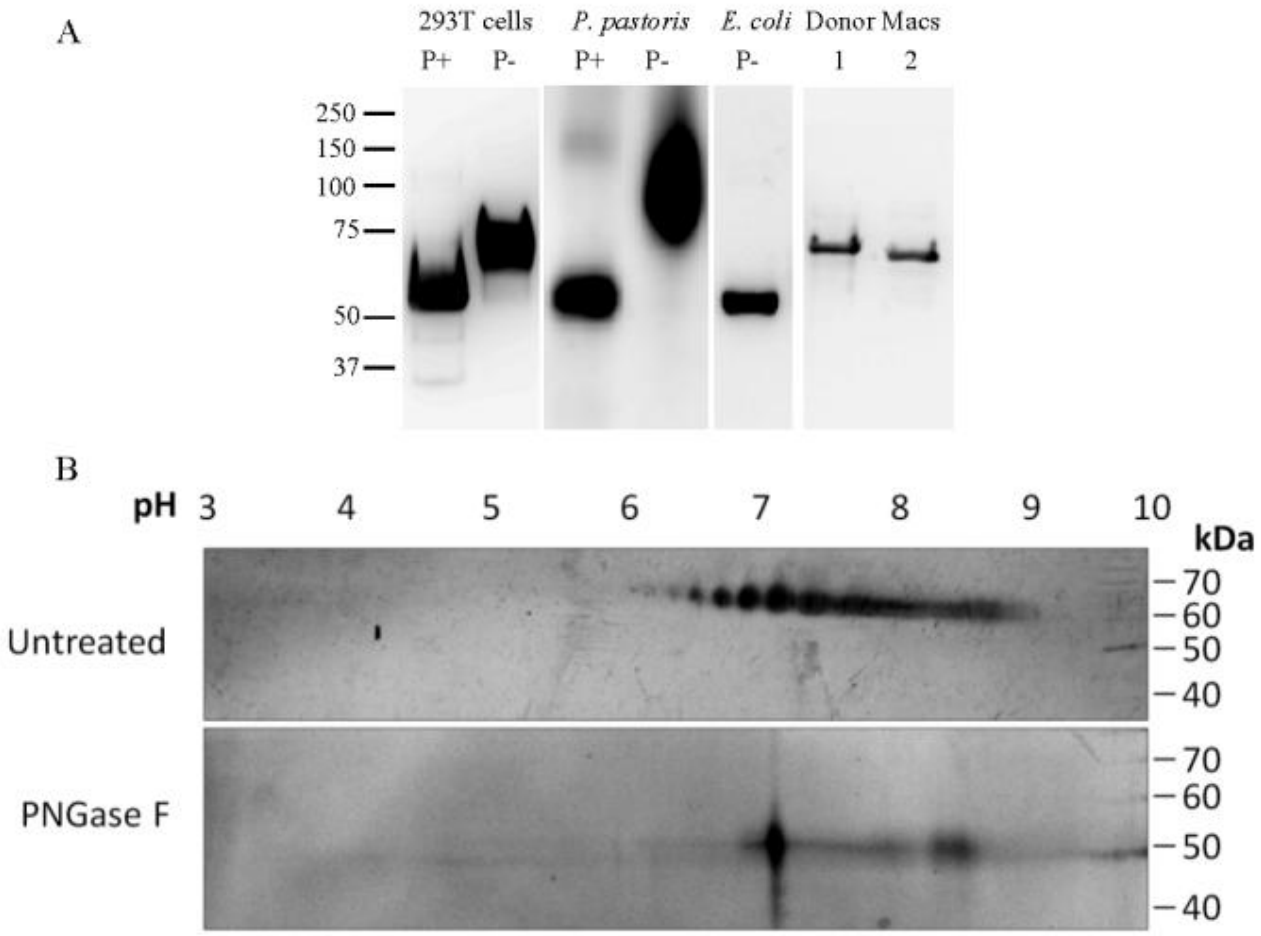

FIGURE 3

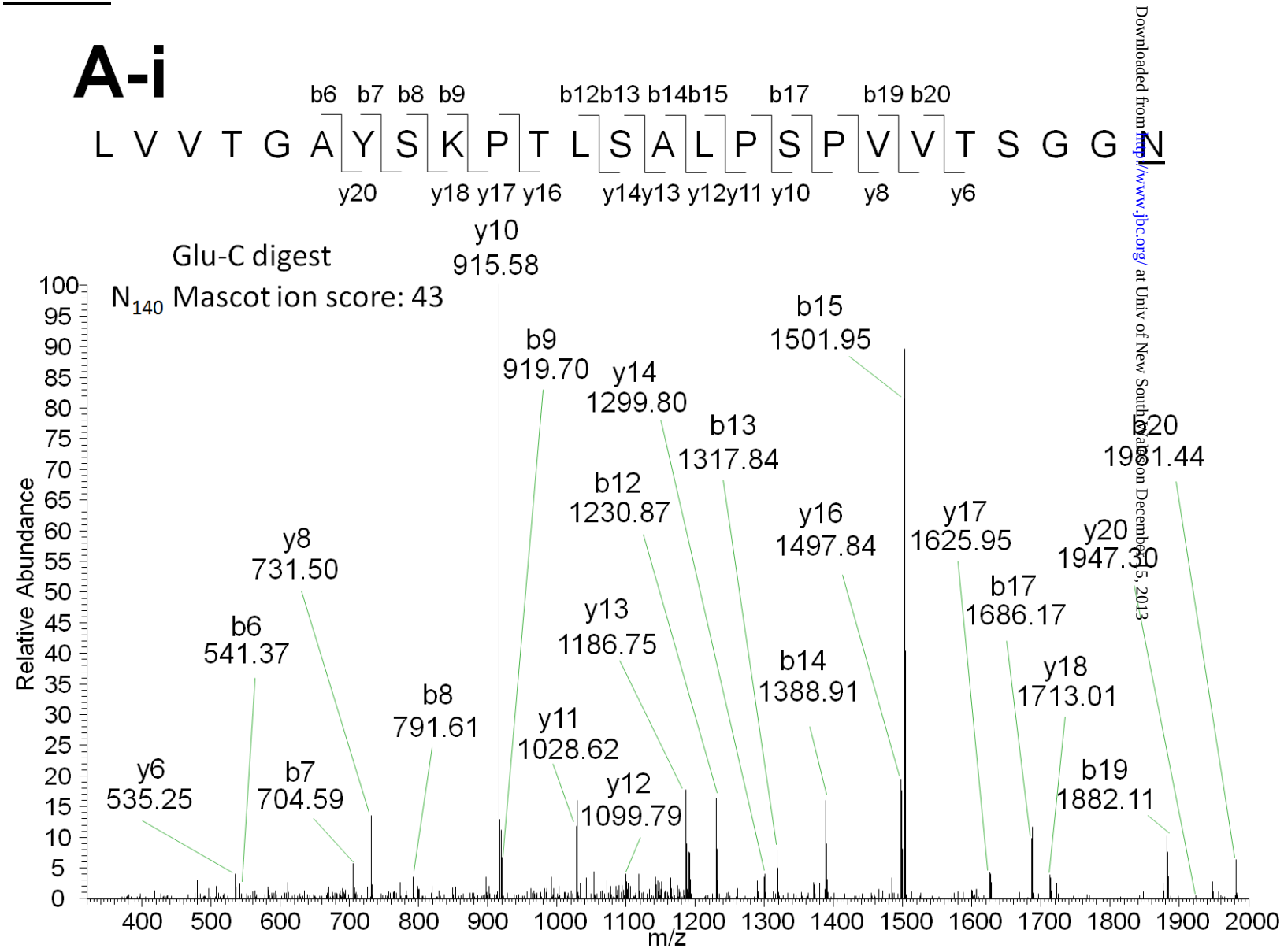

A-ii

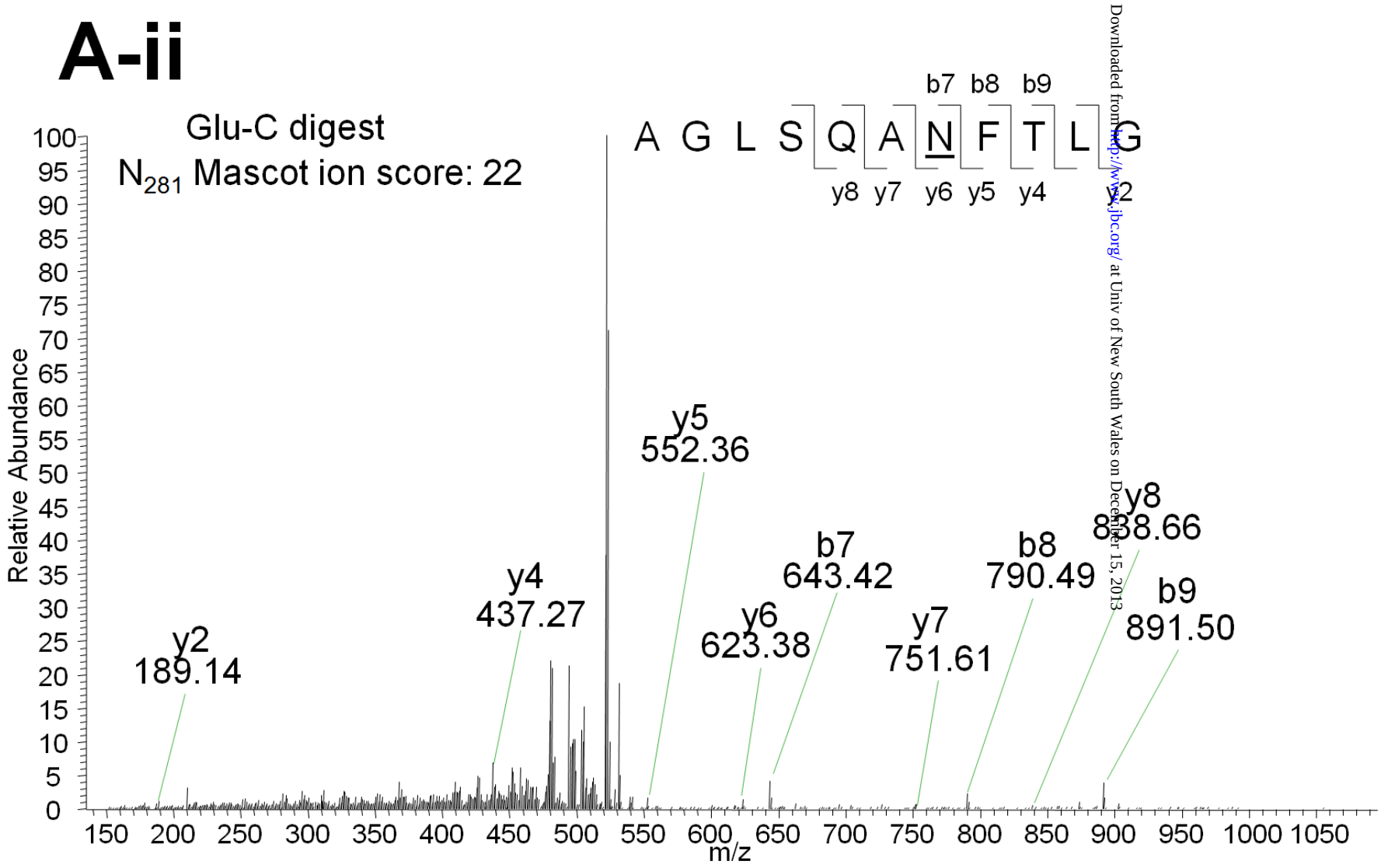

A-iii

Glu-C digest

N_{431} Mascot ion score: 40

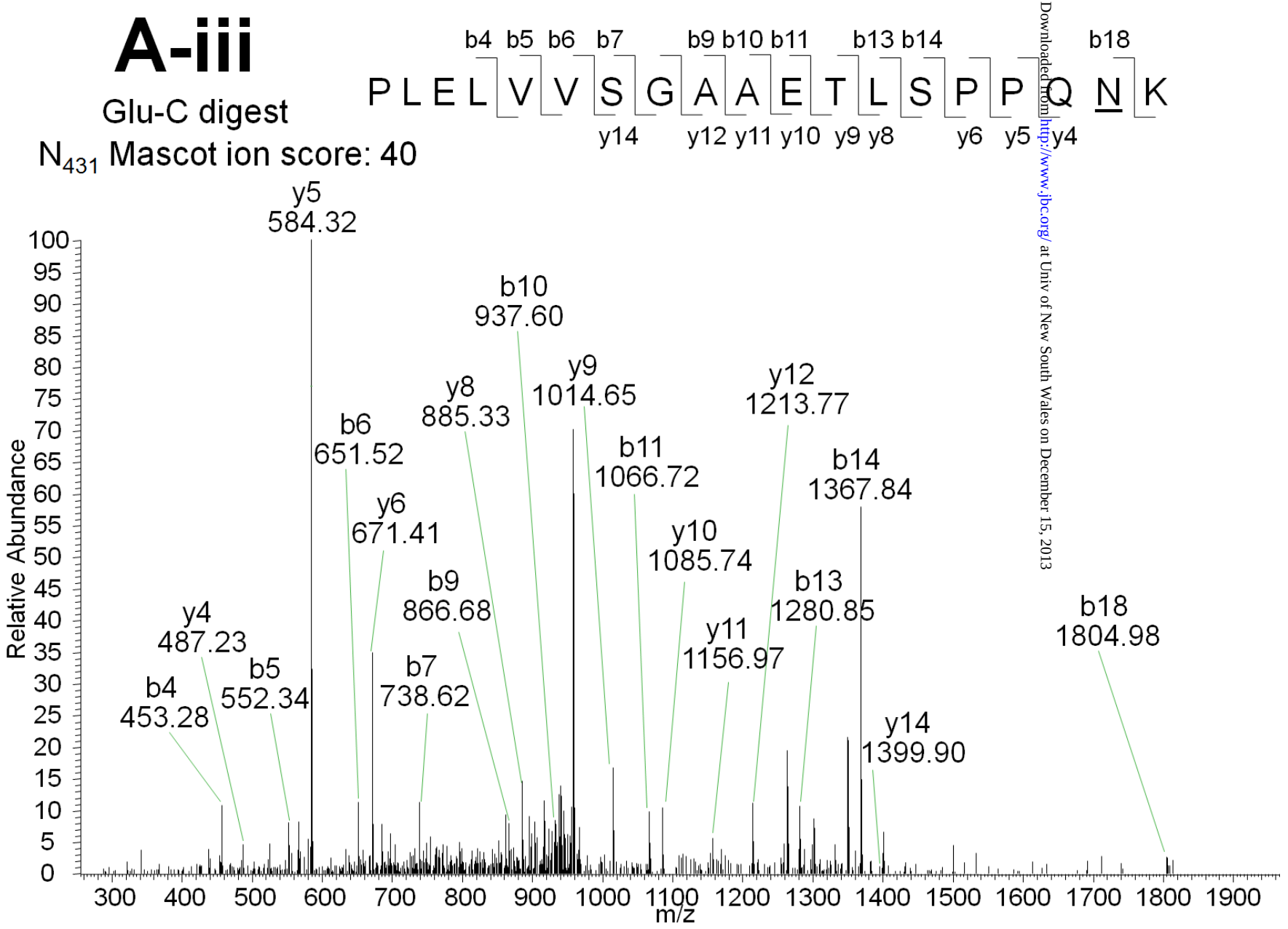

B-i

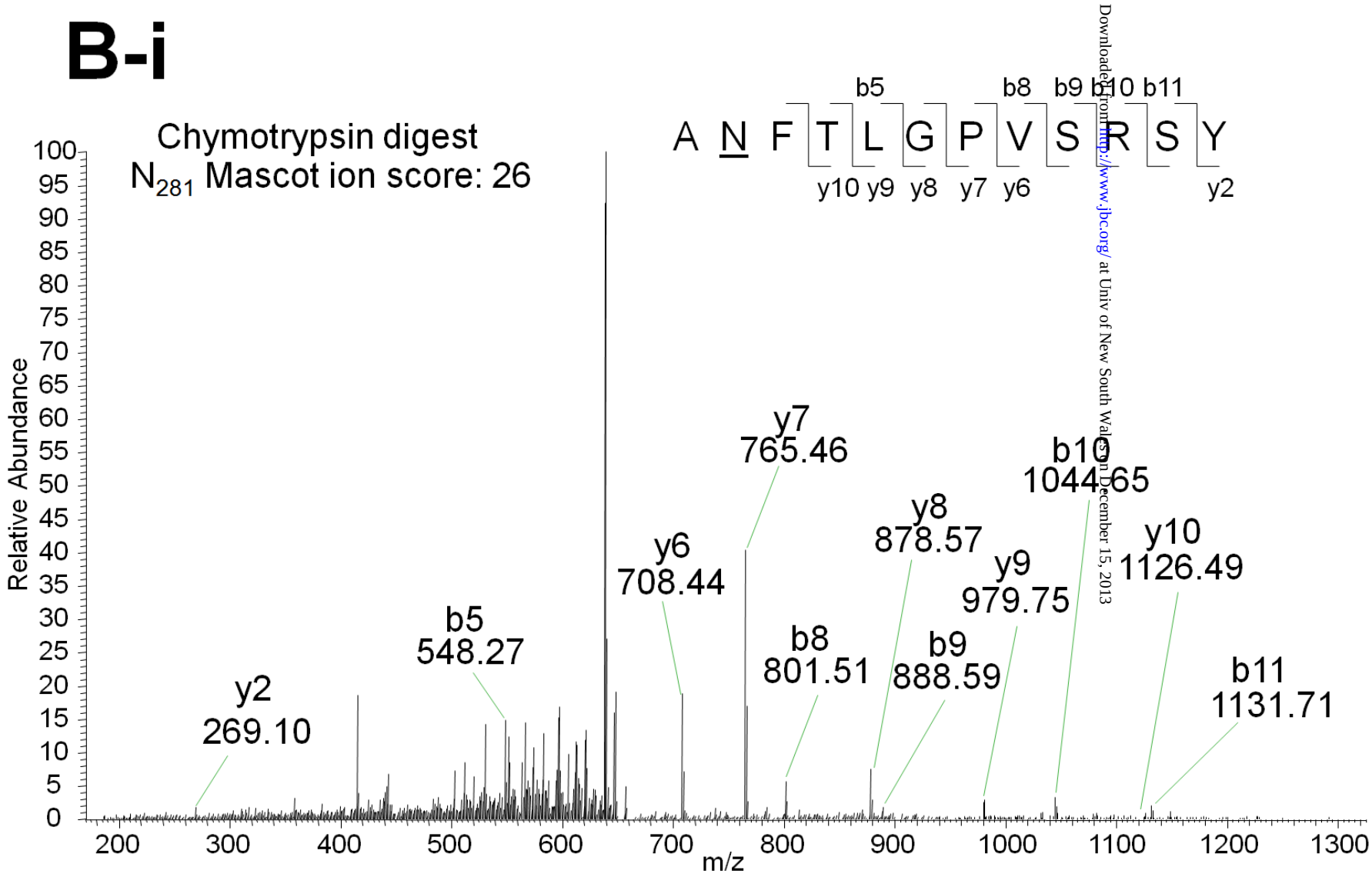

B-ii

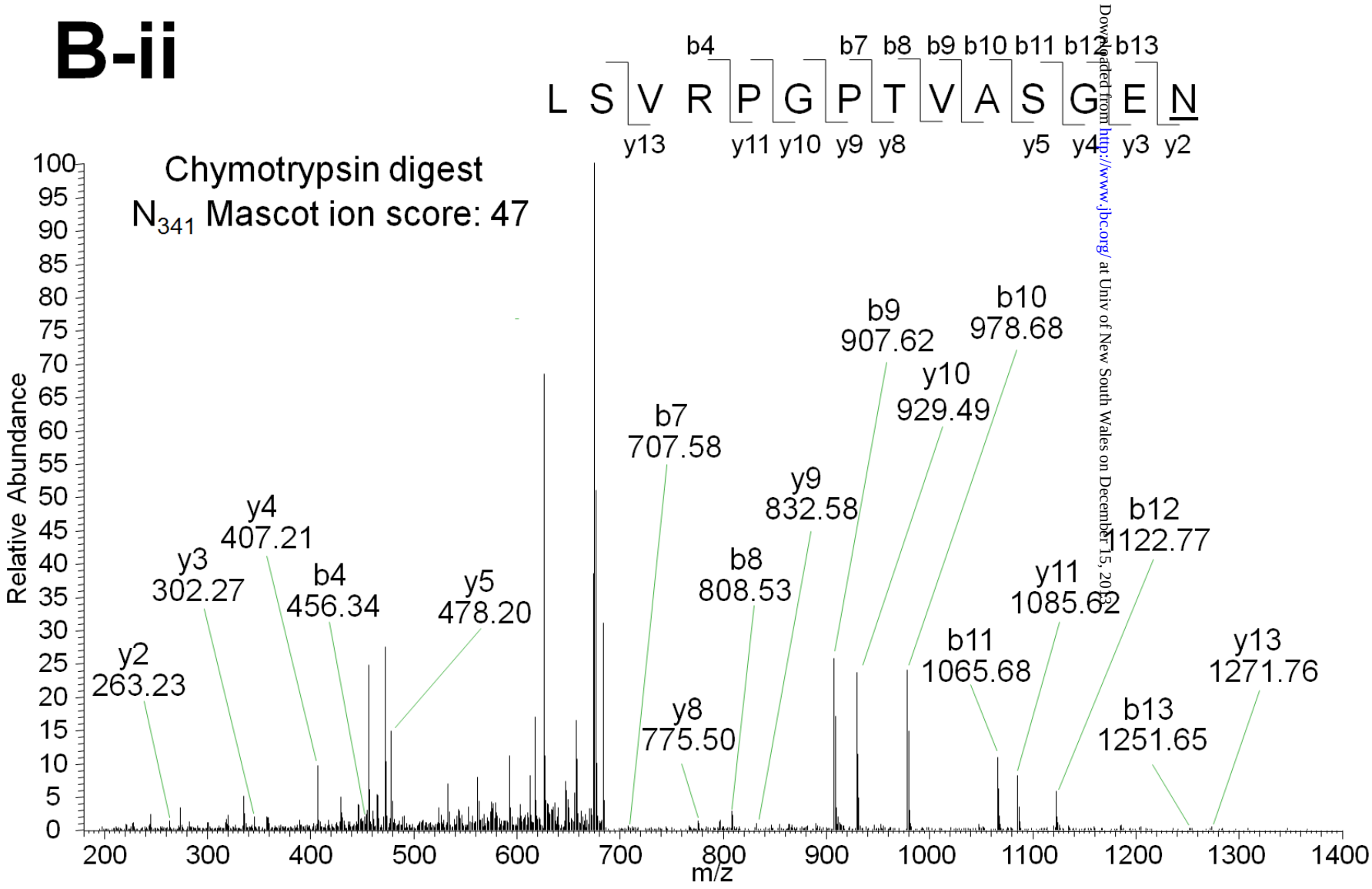

C-i

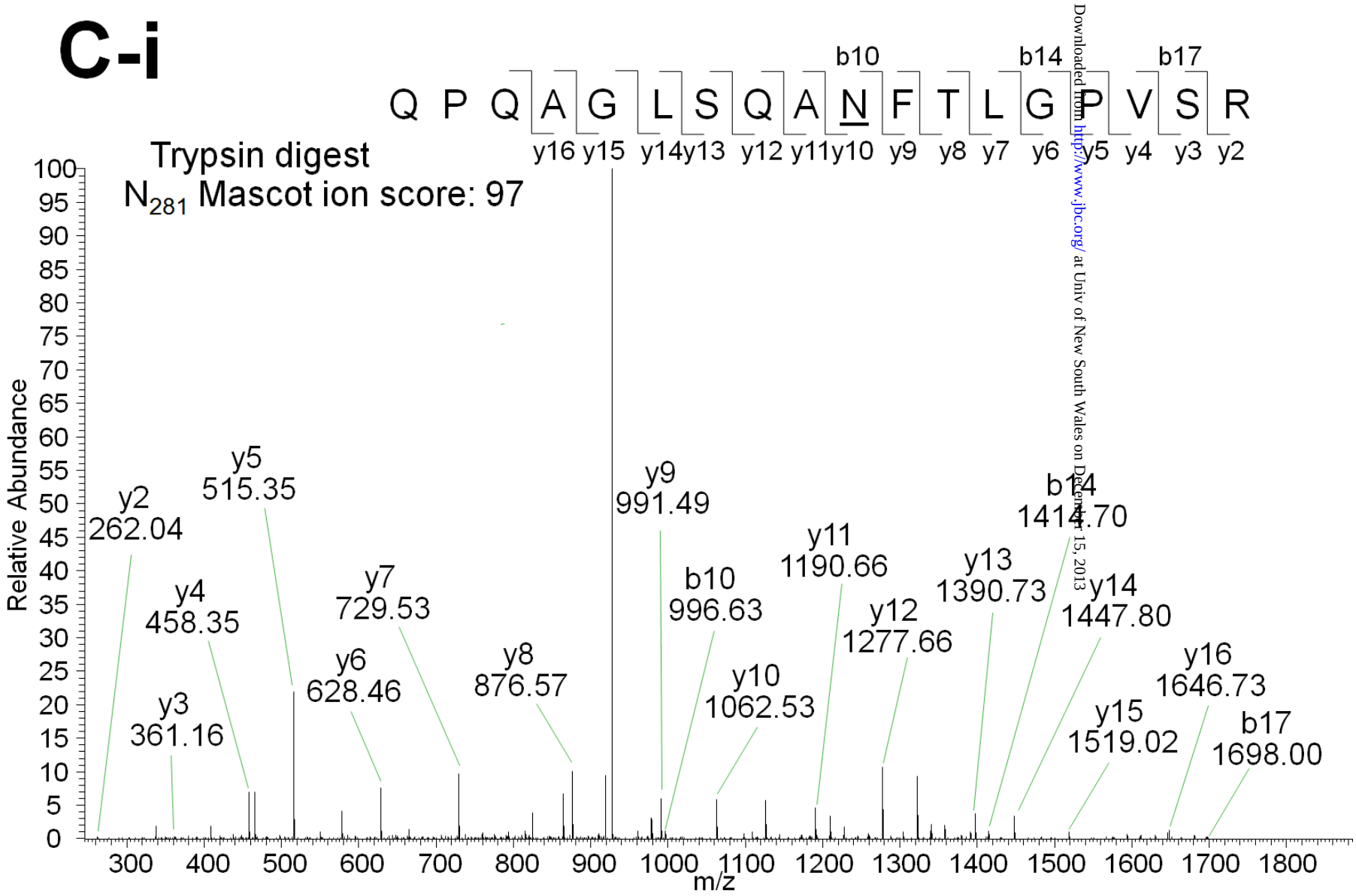

C-ii

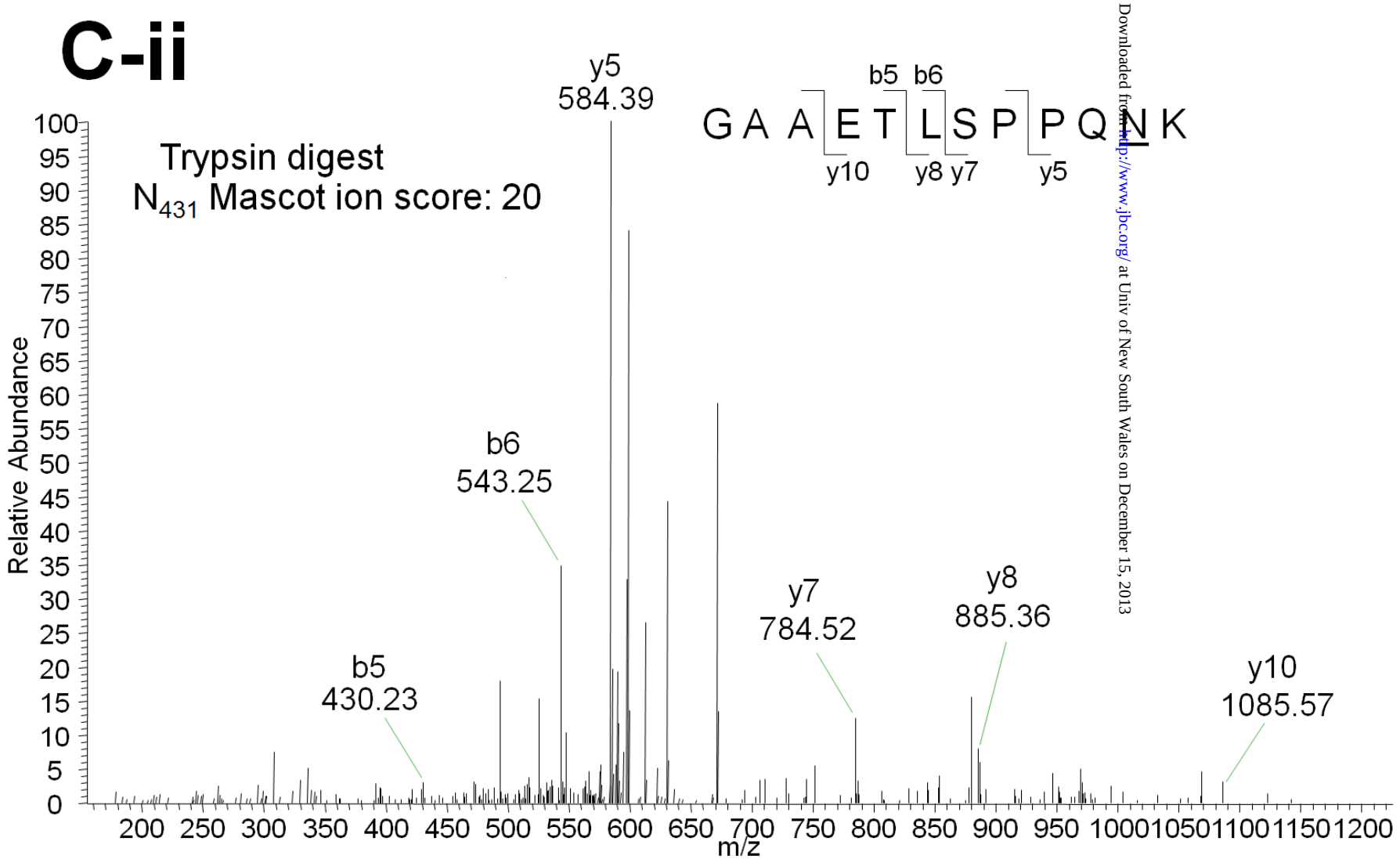

FIGURE 4

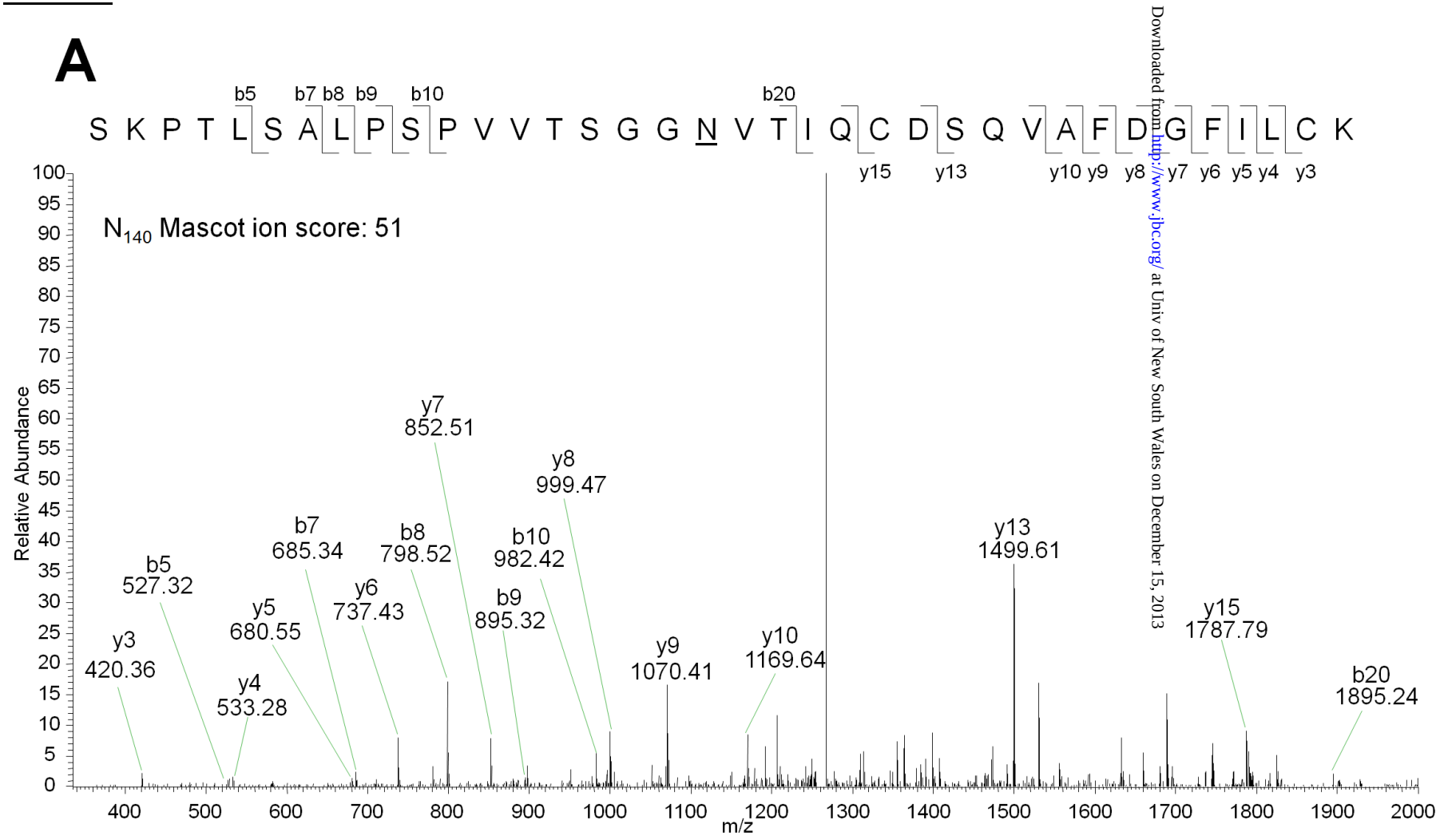

B

N_{281} Mascot ion score: 77

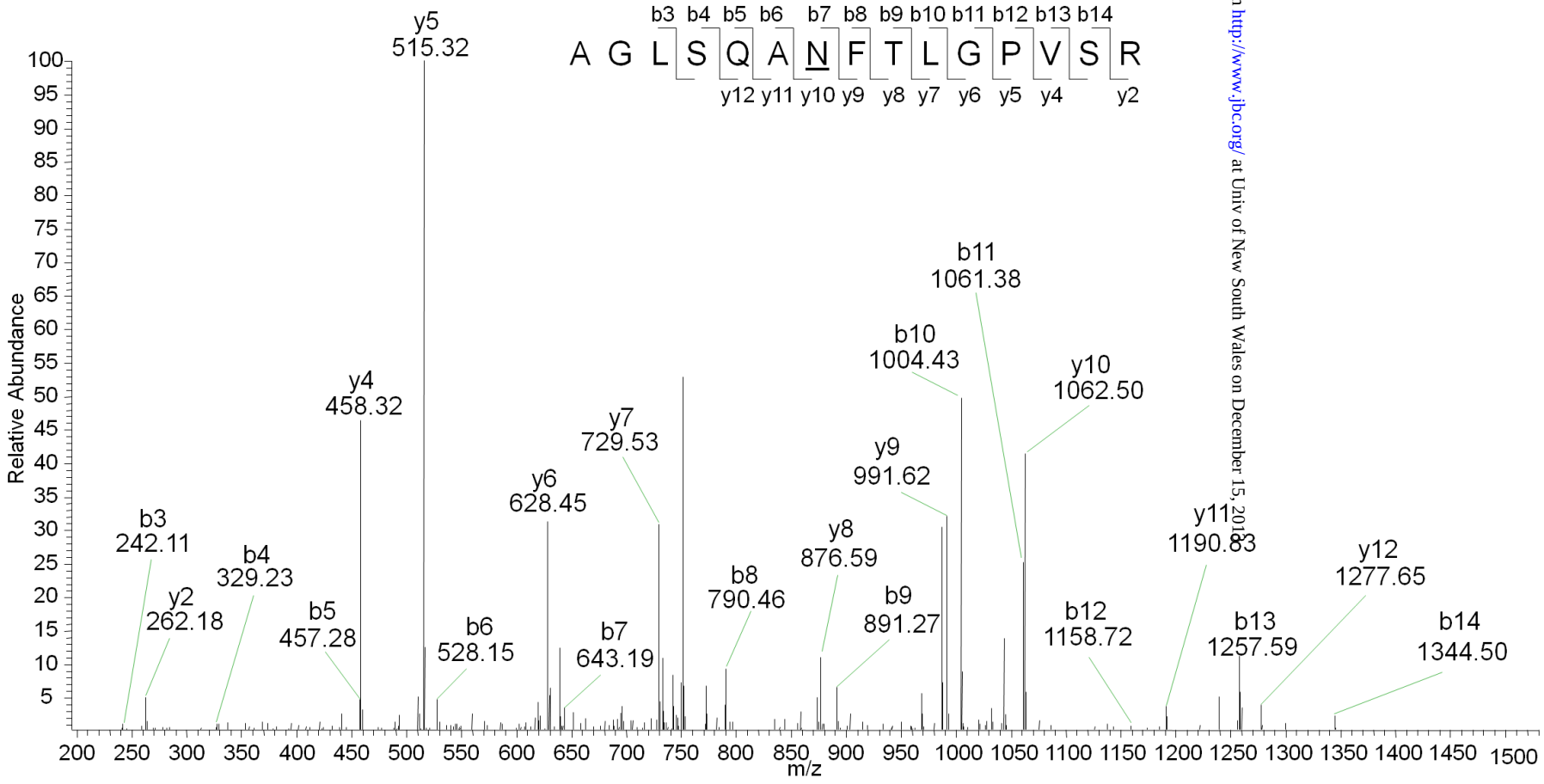

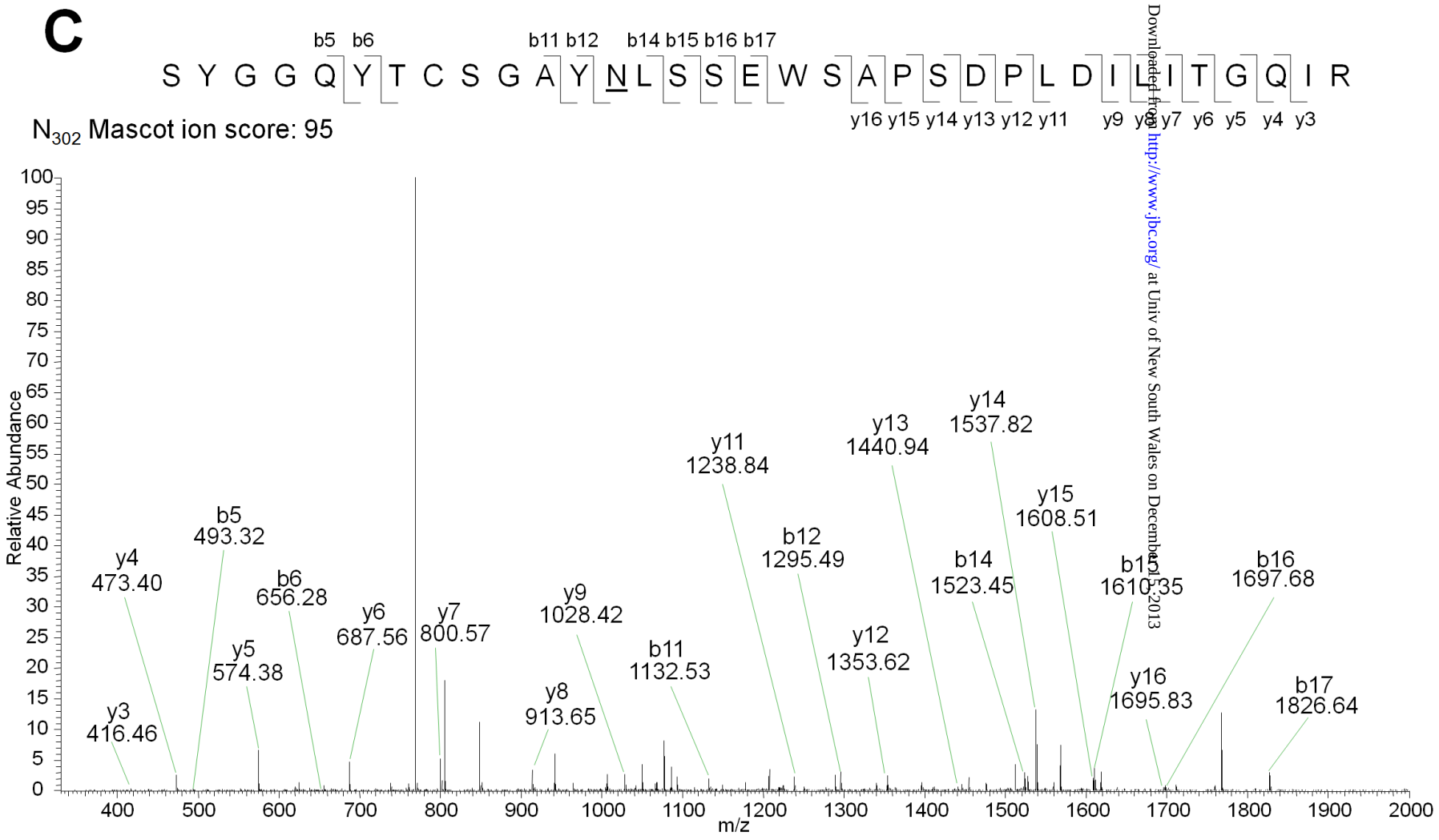

D

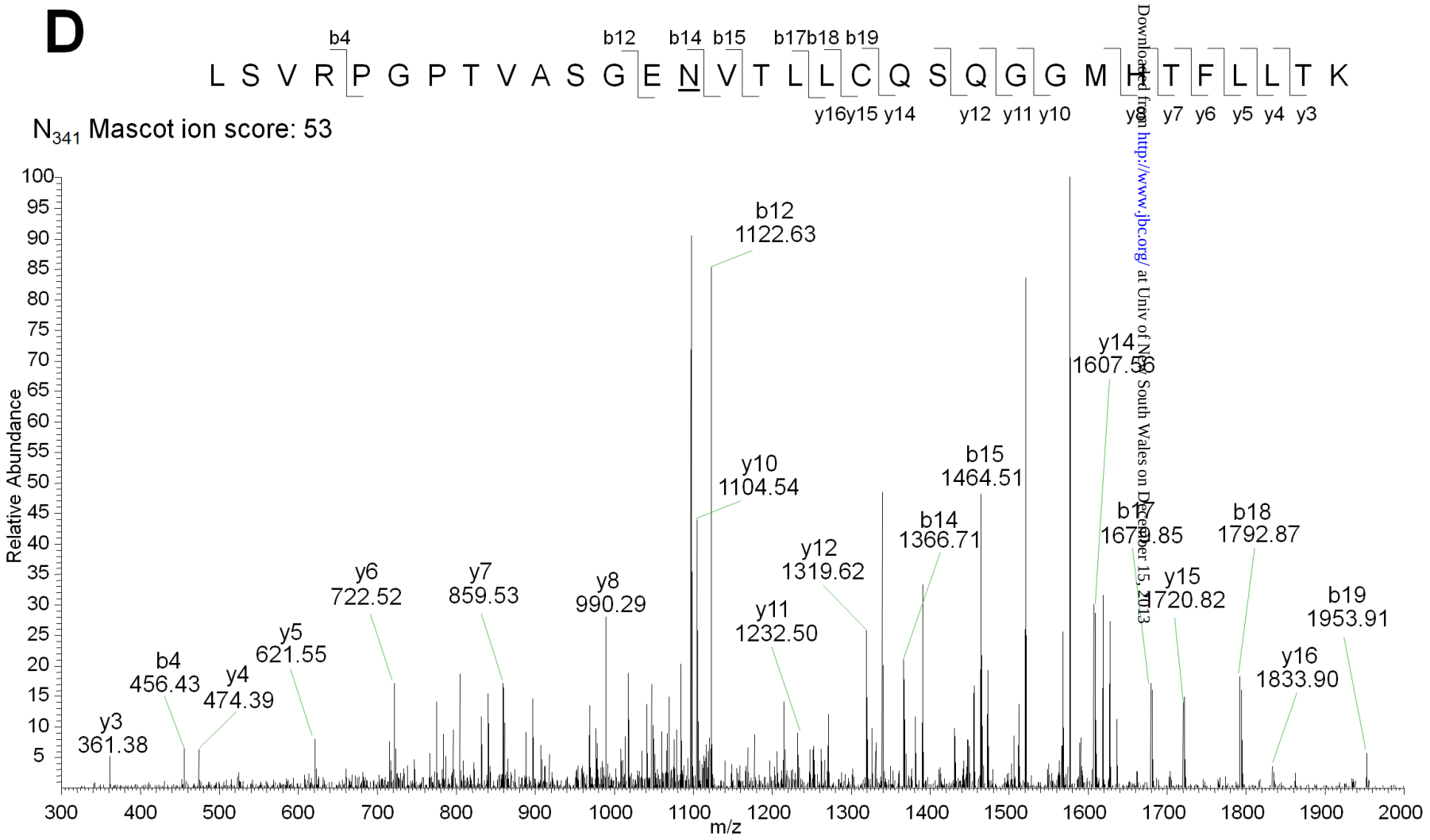

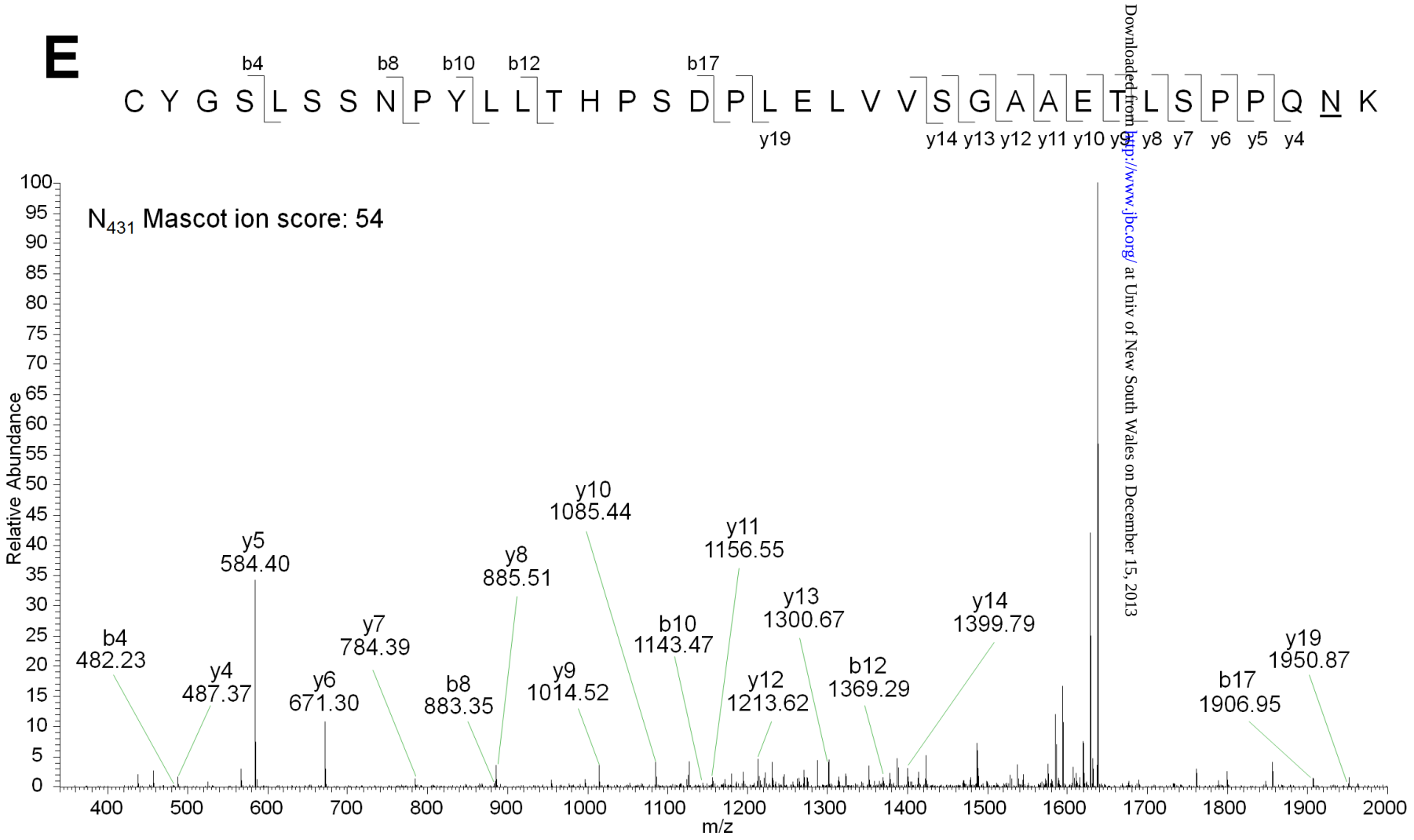

FIGURE 5

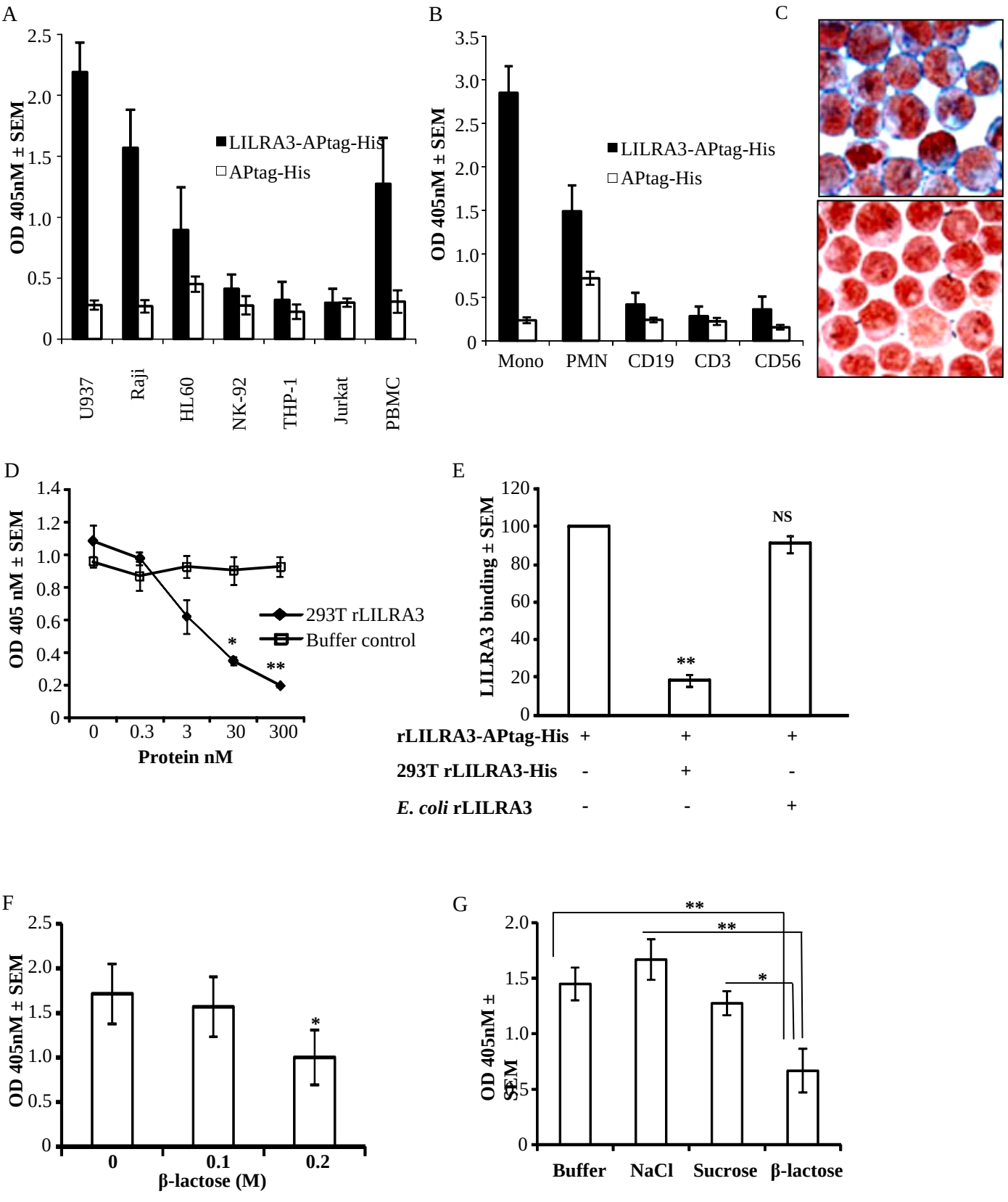

FIGURE 6